Mapping Surface Sequences of the Tubulin Dimer and Taxol-Induced Microtubules with Limited Proteolysis†

José M. de Pereda and José M. Andreu*

Centro de Investigaciones Biológicas, CSIC, Velázquez 144, 28006 Madrid, Spain

Received June 7, 1996; Revised Manuscript Received September 6, 1996⊗

ABSTRACT: Native tubulin αβ dimers and microtubules have been subjected to limited proteolysis with trypsin, chymotrypsin, elastase, clostripain, proteinase lysine-C, thermolysin, protease V8, papain, subtilisin, proteinase K, proteinase aspartic-N, and bromelain. Eighty nicking points have been mapped onto the α- and β-tubulin sequences with the aid of site-directed antibodies, of which 18 sites have been exactly determined by N-terminal sequencing, and the probable position of 6 others deduced from protease specificities. Proteolytic sites cluster into five characteristic zones, including the C termini of both chains. Residues accessible to proteases in the tubulin dimer include α-tubulin Lys40-Thr41-Ile42, Glu168-Phe169-Ser170, Ser178-Thr179-Ala180-Val181, Lys280-Ala281, Glu290-Ile291, Ala294-Cys295, Arg339-Ser340 (plus probably Lys60-His61 and Glu183-Pro184) and β-tubulin Gly93-Gln94, Lys174-Val175, Gly277-Ser278, Tyr281-Arg282-Ala283, Cys354-Asp355 (plus probably Arg121-Lys122, Phe167-Ser168, Tyr183-Asn184, and Glu426-Asp427 or Ala430-Asp431). While the majority of these sites remain accessible at the outer surface of taxol-induced microtubules, α-tubulin Lys280-Ala281, Arg339-Ser340 and β-tubulin Tyr281-Arg282-Ala283 (and probably Arg121-Lys122) become protected from limited proteolysis, suggesting that they are close to or at intermolecular contacts in the assembled structure. The protease nicking points constitute sets of surface constraints for any three-dimensional model structures of tubulin and microtubules. The dimer tryptic site at α-tubulin 339-340 jumps approximately 12−22 residues upstream (probably to Lys326-Asp327 or Lys311-Tyr312) in taxol microtubules, suggesting a tertiary structural change. The cleavage of the approximately 10 C-terminal residues of α-tubulin by protease V8, papain, and subtilisin is inhibited in taxol microtubules compared to tubulin dimers, while the approximately 20 C-terminal residues of β-tubulin are similarly accessible to protease V8, subtilisin, proteinase K, proteinase AspN, and bromelain and show enhanced papain cleavage. This is consistent with models in which the α-tubulin C-terminal zone is near the interdimer contact zone along the protofilaments, whereas the C terminus of β is near the interface between both subunits.

Microtubules are essential for a number of cell functions, including cell motility, intracellular transport, mitosis, and cell shape. The three-dimensional structures of the αβ-tubulin dimer and microtubules are known to low resolution (Amos & Klug, 1974; Mandelkow et al., 1977; Beese et al., 1987; Andreu et al., 1992; Song & Mandelkow, 1995; Kikkawa et al., 1995), and a medium-resolution density map of tubulin in zinc sheets has been presented (Nogales et al., 1995). The high-resolution structure of tubulin and the detailed interaction mechanisms which are responsible for microtubule assembly and microtubule functions are not known [for reviews, see Mandelkow and Mandelkow (1995) and Monasterio et al. (1995)]. On the other hand, the crystal structures of the motor domains of kinesin and the related microtubule-based motor *ncd* have very recently been determined (Kull et al., 1996; Sablin et al., 1996).

Limited proteolysis methods have been used extensively to investigate protein structure, function, and macromolecular complexes (Price & Johnson, 1989; Wilson, 1991; Kruft et al., 1991; Plyte & Kneale, 1994). The restrictions for a given peptide bond to be susceptible to proteolysis in a native protein include the following. (i) The side chains of the amino acid residues forming the bond must satisfy the chemical specificity of the protease (these range from nonspecific to residue-specific). (ii) The bond must be accessible at the surface of the three-dimensional structure of the protein, for example forming part of a loop or a hinge. (iii) The peptide chain is typically flexible so that it may fit into the protease binding site; it frequently lacks a defined secondary structure, although cleavable helical zones are known (Fontana et al., 1986; Hubbard et al., 1991). Therefore, limited proteolysis is very useful for mapping surface bonds of a given protein or macromolecular structure. However, not observing a given potential nicking site does not prove that it is buried within the protein. On the other hand, proteolytic fragments do not necessarily correspond to structural domains, in particular in cases in which they do not spontaneously dissociate.

Actin is a cytoskeletal protein that exists in unassembled (G-actin) and polymerized (F-actin) states, for which both limited proteolysis and high-resolution data are available. The sequence 39−69 of actin is cleaved at several positions by proteases, including trypsin, chymotrypsin, proteinase K, clostripain, and subtilisin among others (Sheterline & Sparrow, 1994). In the atomic structure of G-actin (Kabsch et al., 1990), this zone is in subdomain 2. Most of the nicking points are placed in the DNAse binding loop 39−51, which

† This work was supported in part by DGICyT Grant PB920007 and a predoctoral fellowship from Caja Madrid to J.M.d.P.

* Author to whom correspondence should be addressed. Fax: 34-1-5627518. E-mail: cibjm07@cc.csic.es.

⊗ Abstract published in *Advance ACS Abstracts,* October 15, 1996.

S0006-2960(96)01356-6 CCC: $12.00

is predominantly exposed at the surface of G-actin, and at both ends of the β-strand 65−68. Many of the nicking points in subdomain 2 are protected in F-actin, suggesting that they are occluded upon filament assembly. In the F-actin model proposed by Lorenz et al. (1993), this zone is involved in intermolecular contacts with an adjacent actin monomer, and a local conformational change in the filament structure has been proposed (Lorenz et al., 1993; Fievez & Carlier, 1993).

Limited proteolysis of tubulin has been employed in the past to dissect tubulin structure and function. The acidic C termini of the α- and β-tubulin chains are the main clusters of variability between the different tubulin isoforms, the sites of the known post-translational modifications with the exception of acetylation (Redecker et al., 1994), and the sites of recognition by many of the site-directed antibodies to tubulin and have been implicated in the interactions with MAPs[1] and microtubule motors [for reviews, see Ludueña et al. (1992) and Andreu and de Pereda (1993)]. These flexible zones exposed on the surface of microtubules (Breitling & Little, 1986; de la Viña et al., 1988) can be removed by limited proteolysis with subtilisin (Serrano et al., 1984; Sackett et al., 1985). The cleaved protein exhibits enhanced MAP-independent polymerization ability, possibly due to the reduction of electrostatic repulsion, and readily forms microtubule-like sheets (Serrano et al., 1984), vinblastine-induced spirals (Serrano et al., 1986), zinc sheets (White et al., 1987), and rings (Peyrot et al., 1990). Trypsin predominantly cleaves α-tubulin at arginine 339, while chymotrypsin predominantly cleaves β-tubulin at tyrosine 281 (Mandelkow et al., 1985). Cross-linking with the zero-length reagent 1-ethyl-3-[3-(dimethylamino)propyl]carbodiimide supports a model in which the N-terminal fragment of α-tubulin contacts the C-terminal fragment of β-tubulin in the αβ dimer and (since the dimers are longitudinally aligned along the protofilaments in microtubules) the C-terminal fragment of α-tubulin contacts with the N-terminal fragment of β-tubulin in the protofilaments (Kirchner & Mandelkow, 1985). Limited proteolysis of tubulin by several proteases followed by immunoblotting with anti-peptide antibodies permitted identification of more than 30 proteolytic fragments. The mapped points of cleavage clustered into two well-defined internal zones and the C termini of both chains. Therefore, each tubulin monomer was proposed to consist of three large compact proteolysis resistant regions (each roughly one-third of the chain length each) and the smaller zones accessible to the proteases (de la Viña et al., 1988; Andreu & Arévalo, 1993). However, most of these fragments did not spontaneously dissociate and do not necessarily correspond to the three electron density regions observed in the X-ray fiber diffraction model (Beese et al., 1987), which do not need to be sequential. On the other hand, very few proteolytic sites of tubulin had been sequenced.

In the work reported here, we have employed a panel of 12 commercially available proteases of different specificities to systematically perform comparative limited proteolytic nicking of accessible bonds at the surface of the tubulin dimer and taxol-induced microtubules. Cleavage positions have been mapped on the tubulin sequences, and a number of them have been exactly determined, thus chemically defining a significant number of surface peptide bonds of tubulin in the unassembled and assembled states, as well as potentially interacting zones and local conformational changes.

MATERIALS AND METHODS

Proteins and Chemicals. Tubulin was purified from calf brain and stored in liquid nitrogen, and its concentration was measured spectrophotometrically as described (Weisenberg et al., 1968; Lee et al., 1973; Andreu et al., 1984). Trypsin (type XIII, TPCK-treated, lot 100H8130), α-chymotrypsin (type VII, TLCK-treated, lot 92F8045), clostripain (lot 47F0429), thermolysin (type X, lot 43F0248), and subtilisin Carlsberg (type VIII, lot 54F0230) were from Sigma. Elastase (lot 12573721-11), endoproteinase Lys-C (lots 12291929-22 and 12483825-24), proteinase K (lot 14241922-51), and endoproteinase Asp-N (sequencing grade, lot 14168324−21) were from Boehringer. Protease V8 (from *Staphylococcus aureus*, lot 0301) was from ICN Biomedical. Bromelain (lot 013790) was from Calbiochem, and papain (dried latex) was from Koch-Light Laboratories. Clostripain was dissolved (1 mg/mL) in 10 mM sodium phosphate, 1 mM $CaCl_2$, and 2.5 mM DTT at pH 7.0 and was activated at 25 °C for 2 h. Endoproteinase Lys-C was dissolved to a nominal activity of 20 u/mL in 10 mM sodium phosphate at pH 7.0. Endoproteinase Asp-N was diluted according to the manufacturer's instructions to 0.04 mg/mL in 10 mM Tris-HCl at pH 7.5. Other proteases were dissolved (1 mg/mL) in 10 mM sodium phosphate at pH 7.0 (papain was clarified by centrifugation). Protease aliquots were stored frozen and discarded after use. The reported cleaving specificity of each protease (Bond, 1989) is as follows: trypsin, after Lys or Arg; chymotrypsin, after Trp, Tyr, or Phe; elastase, after uncharged, nonaromatic residues; clostripain, after Arg; endoproteinase Lys-C, after Lys; papain, nonspecific, Arg or Lys preferred; subtilisin, nonspecific, preferably after acid and neutral residues; protease V8, after Glu or Asp; thermolysin, before Leu, Phe, Ile, Val, Met, or Ala; endoproteinase Asp-N, before Asp or cysteic acid; proteinase K, nonspecific, preferably after aromatic or aliphatic residues (Ebeling et al., 1974); and bromelain, nonspecific. The molecular masses quoted for these proteases are between 23 000 and 37 500 Da, except clostripain (53 000 Da) (Products for Protein Biochemistry, Boehringer Mannheim GmbH, P.O. Box 310120, D-6800 Mannheim 31, Germany).

Site-directed antibodies to tubulin [for a review, see Andreu and de Pereda (1993)] and the dilutions employed in immunoblotting were the following. The monoclonal antibody to acetylated Lys40 of α-tubulin (6-11B-1; Le Dizet & Piperno, 1987) was from Sigma and used at 1/10000. Monospecific antibodies to the sequence α(155−168) (NC55) were prepared as described (Arévalo et al., 1990) and used at 1/8000. Monospecific antibodies to the sequence α(214−226) (NC38) were prepared as described (Andreu et al., 1988) and used at 1/10000. Monospecific antibodies to the sequence α(415−445) (C102) were as described (Andreu et al., 1988) and used at 1/3000. The antibody to C-terminal tyrosilated α-tubulin (1A2; Kreis, 1987) was from Sigma

[1] Abbreviations: BSA, bovine serum albumin; DMSO, dimethyl sulfoxide; DTT, 1,4-dithiothreitol; ECL, enhanced chemiluminescence Western blotting detection reagents (Amersham Life Science); EDTA, ethylenediaminetetraacetic acid; MAPs, microtubule-associated proteins; PAGE, polyacrylamide gel electrophoresis; PBS, phosphate-buffered saline (8.1 mM disodium phosphate, 1.5 mM potassium phosphate, 137 mM sodium chloride, and 2.7 mM potassium chloride); PMSF, phenylmethanesulfonyl fluoride; SDS, sodium dodecyl sulfate; Tris, tris(hydroxymethyl)aminomethane; TBS, Tris-buffered saline (10 mM Tris-HCl and 150 mM NaCl at pH 7.4); TLCK, N^{α}-*p*-tosyl-L-lysine chloromethyl ketone; TPCK, *N*-tosyl-L-phenylalanine chloromethyl ketone.

and used at 1/10000. The monoclonal antibody to the amino-terminal sequence $\beta(1-13)$ (P11E12C3) (C. de Inés, G. Pucciarelli, D. Andreu, and I. Barasoaín, Centro de Investigaciones Biológicas, unpublished) was used at 1/50000. The monospecific antibodies to the sequence $\beta(153-165)$ (C140) were as described (Arévalo et al., 1990) and used at 1/100000. The monospecific antibodies to the sequences β-(241−256) (C99) and $\beta(412-431)$ (C106) were as described (Andreu et al., 1988) and employed at 1/2000 and 1/5000, respectively. All these antibodies were tested and found to be α- or β-tubulin-specific in every immunoblot.

Taxol (paclitaxel) was a gift from the late Dr. Matthew Suffness, National Cancer Institute, National Institutes of Health. GTP (dilithium salt) was from Boehringer. PMSF was from Calbiochem. SDS, EDTA, and iodoacetamide were from Sigma. Tween 20 was from Fluka. Other analytical grade reagents were from Merck.

Limited Proteolysis. Tubulin was rapidly equilibrated in 10 mM sodium phosphate and 0.1 mM GTP at pH 7.0 employing Sephadex G-25 (20 × 0.9 cm) columns. $MgCl_2$ (6 mM) was added (final pH of 6.7), and the protein was centrifuged at 100000*g* during 30 min at 4 °C. The tubulin concentration in the supernatant was adjusted to 20 μM, and GTP was added up to 1 mM. Taxol (20 μM) was added in order to assemble microtubules. The residual concentration of DMSO from the taxol stock solution was lower than 0.5% (v/v). An equal concentration of DMSO was added to an identical aliquot of tubulin without taxol. Both were heated at 37 °C during 30 min to induce polymerization of the taxol-containing samples. Then they were incubated with each protease at the indicated weight ratios for 20 min at 25 °C (thermolysin experiments included additional 2 mM $CaCl_2$ in the buffer). The reaction was stopped by adding an excess of protease inhibitor. PMSF (2 mM) was used to inhibit trypsin, chymotrypsin, elastase, subtilisin, protease V8, papain, endoproteinase Lys-C, and proteinase K; iodoacetamide (2 mM) was used to inhibit clostripain and bromelain. EDTA (2 mM) was used to inhibit thermolysin and endoproteinase Asp-N. An equal volume of SDS electrophoresis sample solution (de la Viña et al., 1988) was immediately added, and the samples were boiled.

Sedimentation velocity measurements of tubulin solutions (with 0.1 mM GTP) were performed with a Beckman Optima XLA analytical ultracentrifuge, employing double-sector cells in an AnTi rotor at 60 000 rpm and 25 °C. The cells were scanned at 295 nm, and the weight average sedimentation coefficients were measured employing the second-moment method as described (Laue et al., 1993), with Origin software supplied by Beckman.

Microtubule assembly was monitored turbidimetrically at 350 nm, and the concentrations of polymers and of non-polymerized tubulin were determined by the sedimentation assay described by Díaz and Andreu (1993), with the following minor modifications. Samples were warmed at 37 °C for 1 h and centrifuged at 100000*g* for 10 min at 37 °C in a Beckman TLA-100 rotor; alternatively, samples were warmed at 37 °C for 30 min, then kept at 25 °C for 20 min, and centrifuged at 25 °C as above. The morphology of the polymers was observed by electron microscopy of negatively stained samples as described (Díaz & Andreu, 1993).

Electrophoresis, Immunoblotting, and N-Terminal Microsequencing. Samples were analyzed by SDS-PAGE (Laemmli, 1970) with modifications (Best et al., 1981), employing 10% acrylamide pH 9 resolving gels, and peptide bands were stained with Coomassie blue (de la Viña et al., 1988). Alternatively, peptides were electrophoretically transferred onto membranes in a semidry Trans-Blot apparatus (Bio-Rad), using as transfer buffer 25 mM Tris, 192 mM glycine, and 20% (v/v) methanol at pH 8.5. Nitrocellulose sheets (0.2 μm, Bio-Rad) were used for immunoblotting, whereas poly(vinyldene difluoride) (PVDF) sheets (Immobilon-P^{SQ}, Millipore) were used for microsequencing (Matsudaira, 1987). The apparent molecular masses of proteolytic tubulin fragments were calculated, employing as molecular mass markers (Bio-Rad) phosphorylase *b* (M_r = 97 400 Da), BSA (M_r = 66 200 Da), ovalbumin (M_r = 45 000 Da), carbonic anhydrase (M_r = 31 000 Da), soybean trypsin inhibitor (M_r = 21 500 Da), and lysozyme (M_r = 14 400 Da). Immunoblotting of the proteolytic fragments was performed as described (Andreu et al., 1988) with the following modifications. Nitrocellulose sheets were incubated in 1% gelatin−PBS overnight at room temperature and then briefly rinsed with PBS-T (PBS containing 0.05% v/v Tween 20). Sheets were incubated with site-directed antibodies diluted in PBS-T containing 0.5% BSA for 1.5−2 h at room temperature and washed three times with PBS-T. In order to detect monospecific primary antibodies, sheets were incubated with peroxidase-conjugated mouse anti-rabbit immunoglobulin (Bio-Rad) diluted 1/10000 in PBS-T containing 0.5% BSA for 1.5 h and washed four times with PBS-T and twice with PBS. Sheets were then incubated for 1 min with the enhanced chemiluminescence reagents (ECL, Amersham), and Kodak X-Omat film was exposed to them for 30 s to 3 min. When monoclonal primary antibodies were employed, dilutions were made in TBS instead of PBS and they were detected with peroxidase-conjugated goat anti-mouse immunoglobulin (Bio-Rad) diluted 1/10000 in TBS-T containing 0.5% BSA.

Polypeptides blotted onto Immobilon-P^{SQ} membranes were stained with Coomassie blue and stored as described (Matsudaira, 1987). N-Terminal Edman microsequencing of the peptides adsorbed onto the membranes was performed on an Applied Biosystems 477A sequencer equipped with on-line HPLC analysis of the phenylthiohydantoin derivatives. This procedure works for a number of majority or contaminant-free peptides.

Since the apparent (electrophoretic) molecular mass of the tubulin chains and their fragments is anomalous (de la Viña et al., 1988), in order to obtain more accurate estimates, a procedure based on the use of sequenced tubulin fragments as internal standards was employed. The apparent molecular mass of well-known fragments was plotted versus their theoretical molecular mass (calculated from their sequence, without taking into account the possible increase due to post-translational modifications, whose exact extension is not known). This clearly gave nonlinear plots, which were arbitrarily fitted employing third-order polynomials (not shown). Four types of peptides were defined: α-tubulin fragments containing its N-terminal sequence (i) or the C-terminal sequence (ii) and β-tubulin fragments containing its N-terminal sequence (iii) or the C-terminal sequence (iv). This classification takes into account the different electrophoretic mobility of α- and β-tubulin and the different amino acid composition of the terminal regions in each chain. The corrected value of the apparent molecular mass of the unknown fragments in each class was obtained by interpolation.

Table 1: Amino Terminal Sequences of Limited Proteolysis Fragments of Tubulin

protease	sample[a]	fragment			
		name	amino sequence	position in sequence[b]	theoretical M_r[b]
trypsin	DM	TRα1	M-E-I-I	1−339	37 520
	DM	TRα4	SIQFV	340−451	12 576
	MT	TRβ1	V-DTVVEP	175−445	30 887
	DM	TRβ1	V- - - VV	175−445	30 887
	MT	TRβ4	M-EIV-IQ	1−174	18 986
chymotrypsin	MT	CHα1	SIYPAPQVS	170−451	31 529
	DM	CHβ2	-ALTVP-L	282−445	18 913
elastase	DM	ELα1	TAVV	179−451	30 585
	DM	ELα3	-FEPANQMVK	295−451	17 615
	DM	ELβ1	MREIV	1−354	39 326
	DM	ELβ2	DIPP-GLK	355−445	10 547
clostripain	DM	CLα3	-IQFV	340−451	12 576
	DM	CLβ5	AL-VP-G-QQM	283−445	18 757
Lys-C	MT	LCα1	TIGGGDDS	41−451	45 679
	DM	LCα1	TIGGG	41−451	45 679
	DM	LCα2	MRE-ISI	1−280	30 953
	DM	LCα3	TIGGGDDS	41−280	26 555
	DM	LCα5	AY-EQL-VAEI	281−451	19 143
thermolysin	MT	THα1	IGG-DD-F	42−451	45 578
	DM	THα1	- - - - DD	42−451	45 578
protease V8	DM	V8α1	F-IYPAPQ	169−451	31 676
	MT	V8α1	FSIYPA	169−451	31 676
	MT	V8α4	IT-A-FEP	291−451	18 014
	DM	V8α4	I-NA-FE	291−451	18 014
papain	DM	PAα4	-AVVEPY	179−446 ± 4	nd
subtilisin	DM	SBα3	MREI-I- -H	1−266 ± 31	nd
	DM	SBα4	- - EPYNSI	181−442 ± 5	nd
proteinase K	DM	Kβ4	MREI	1−285 ± 24	nd
bromelain	MT	BRβ2	Q-GAGNN-A	94−438 ± 6	nd
	MT	BRβ7	SQQYRA	278−407 ± 13	nd

[a] Tubulin heterodimer (DM) or taxol-induced microtubule (MT) samples were employed for sequencing. [b] Position in the sequence and theoretical M_r determined according to the pig brain sequences.

Mapping of Tubulin Proteolytic Fragments. The experimentally determined N-terminal peptide sequences were assigned directly by comparison with the complete porcine brain α- and β-tubulin sequences (Krauhs et al., 1981; Ponstingl et al., 1981), employing a personal computer program, and the complementary fragments produced by the same cleavage were identified. We found no difference between the bovine and porcine brain tubulin sequences at the positions examined. In this way, a number of cleavage points were precisely determined. The rest of the fragments were identified only from their reactivity with the site-directed antibodies, and their extension was measured from their corrected molecular mass values (employing the actual tubulin sequences instead of average residue molecular mass values). It should be noted that mass spectrometry, which has been fruitfully used to investigate post-translational modifications of tubulin (Redecker et al., 1994; Alexander et al., 1991), might be employed to map proteolysis fragments. However, this was hampered by the microheterogeneity of the tubulin chains, which reduces the resolution of direct molecular mass determination (Rüdiger et al., 1995), and by the fact that we have not as yet found a convenient HPLC method for separation and identification of the tubulin chains and their fragments.

RESULTS AND DISCUSSION

Tubulin Dimer and Microtubule Samples Subjected to Comparative Limited Proteolysis. Purified calf brain tubulin was proteolyzed in 10 mM sodium phosphate buffer, 6 mM $MgCl_2$, 1 mM GTP, and pH 6.7 buffer at 25 °C. Since Mg^{2+} ions are known to induce tubulin self-association, the degree of incipient oligomerization of tubulin under our conditions

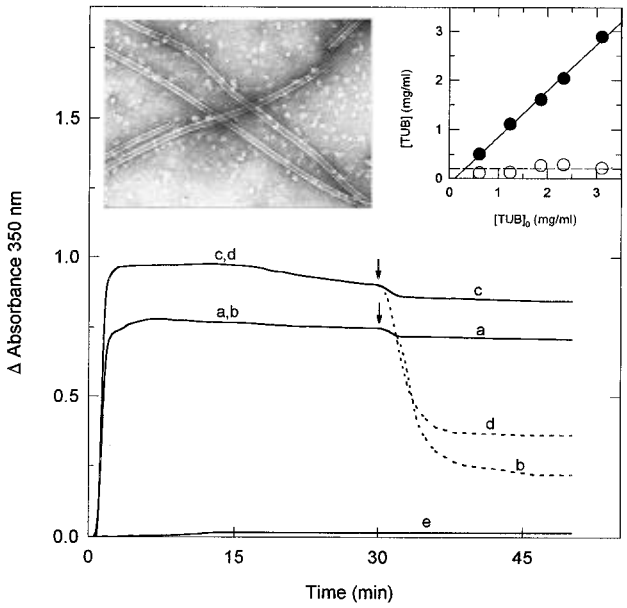

FIGURE 1: Turbidimetric time course of assembly of 20 μM tubulin induced by 20 μM taxol, in 10 mM sodium phosphate, 1 mM GTP, and 6 mM $MgCl_2$ at pH 6.7 and 37 °C (lines a and b) or in the same buffer with the addition of 2 mM $CaCl_2$ (lines c and d). Arrows indicate cooling of the samples to 20 °C (solid lines a and c) or 2 °C (dashed lines b and d). Left inset: electron micrograph of negatively stained taxol-induced microtubules, assembled at 37 °C and left at 20 °C for 25 min. Right inset: quantification by sedimentation of the microtubule assembly induced by taxol. Solid circles, pelleted tubulin; open circles, tubulin in supernatant.

was evaluated by sedimentation velocity. The weight average sedimentation coefficient of 20 μM tubulin in the absence of Mg^{2+} had an uncorrected $s_{20,w}$ value of 5.4 S,

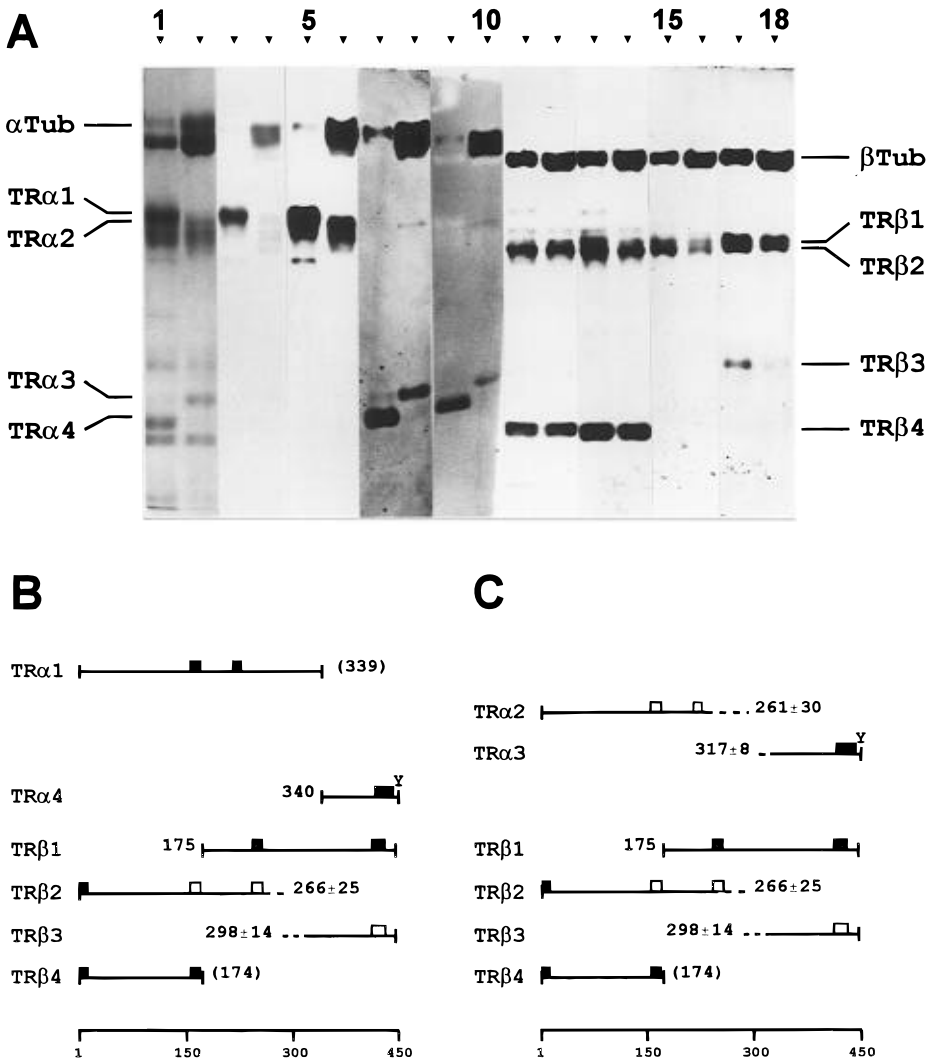

FIGURE 2: Limited proteolysis of tubulin and taxol-induced microtubules by trypsin (TPCK-treated, 1% w/w ratio to tubulin). Panel A: lanes 1, 3, 5, 7, 9, 11, 13, 15, and 17, heterodimeric tubulin; lanes 2, 4, 6, 8, 10, 12, 14, 16, and 18, taxol-induced microtubules. Lanes 1 and 2 are a Coomassie blue-stained gel portion. Lanes 3 to 18 are immunoblots with the following site-directed antibodies: antiα(155−168), lanes 3 and 4; antiα(214−226), lanes 5 and 6; antiα(415−430), lanes 7 and 8; 1A2 lanes 9 and 10; antiβ(1−13), lanes 11 and 12; antiβ(153−165), lanes 13 and 14; antiβ(241−256), lanes 15 and 16; and antiβ(412−431), lanes 17 and 18. Each of these immunoblots included a nonproteolyzed tubulin sample in this and every following experiment (not shown). Marks on both sides indicate the position of α- and β-tubulin and their fragments. Panels B and C: schemes of fragments produced by trypsin-limited proteolysis of heterodimeric tubulin (B) and taxol-induced microtubules (C). The reaction of each band with the site-directed antibodies in the original immunoblots is indicated by solid rectangles (strong signals) and open rectangles (comparatively weak signals for a given antibody; note that some of the antibodies are extremely sensitive). The reaction of the C-terminal tyrosine with the 1A2 antibody is indicated by the letter Y. These reactivities are employed to align each fragment on the sequences. Numbers indicate the ends of the fragments by reference to the pig brain tubulin sequences. These numbers are given without error when they come from N-terminal sequencing; errors are given for tubulin fragment sizes estimated from corrected electrophoretic molecular masses; parentheses indicate either a carboxy-terminal residue assigned by being complementary to a sequenced N-terminal fragment or an amino-terminal end deduced from a known protease residue specificity. Dashed lines indicate the limits to the position of the fragments.

corresponding to the $s^\circ_{20,w}$ of 5.8 S for the tubulin $\alpha\beta$ dimer (Frigon & Timasheff, 1975; Andreu & Muñoz, 1986), while in the complete buffer (with 0.1 mM GTP), the value was 6.5 S. A previous incubation at 37 °C for 30 min (the conditions required to assemble the parallel microtubule samples) did not increase the later value significantly. The concentrations of oligomers and the apparent equilibrium association constant were estimated by direct application of the model of Mg^{2+}-induced tubulin isodesmic self-association (Frigon & Timasheff, 1975; $s_1 = 5.4$ S, C = 2 mg mL^{-1}). It was concluded that the sedimentation coefficient value observed with Mg^{2+} indicated a mixture of approximately 72.5% tubulin $\alpha\beta$ dimers, 21.5% tetramers, 4.8% hexamers, and insignificant proportions of higher-order oligomers. Considering that the Mg^{2+}-induced self-association of the tubulin $\alpha\beta$ dimer leading to double-ring formation is head to tail (Mandelkow et al., 1983; Díaz et al., 1994), one-half and one-third of the longitudinal contact surfaces are respectively exposed in tetramers and hexamers so that approximately 85% of the tubulin α and β subunits have the same exposed surface as in the 5.8 S heterodimer. Therefore, the tubulin solution was considered qualitatively heterodimeric for the purpose of limited proteolysis. The circular dichroism spectra of these samples, and of 2 mM $CaCl_2$-containing samples, were compared to spectra of samples without 6 mM $MgCl_2$ and found to be identical within experimental error (not shown; the experimental reproducibility of the spectral extremes at 192, 210, and 220 nm was ±4.4, 1.5, and 1.4%, respectively). Therefore, the average secondary structure of tubulin was considered insignificantly modified by the divalent cations added in the limited proteolysis experiments. When in another control

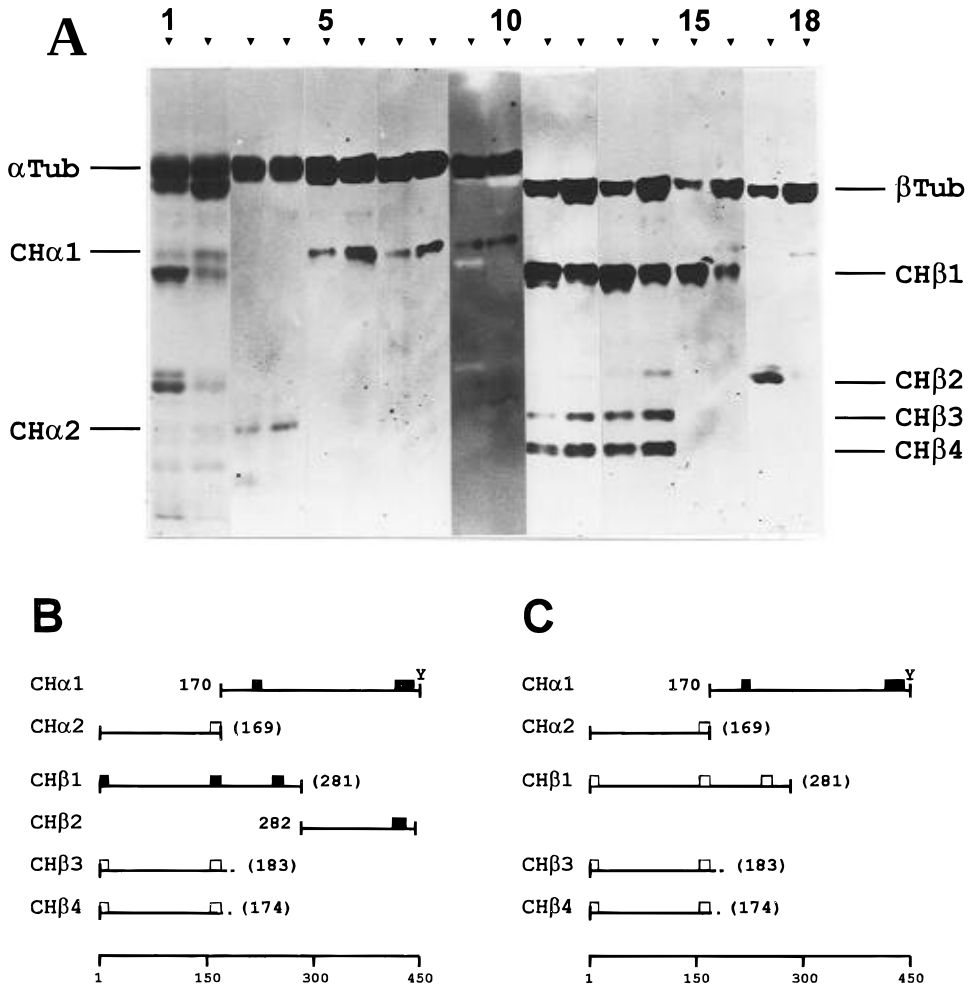

FIGURE 3: Limited proteolysis of tubulin and taxol-induced microtubules by chymotrypsin (TLCK-treated, 2% w/w). Panel A: Coomassie-stained lanes and immunoblots, in positions identical to those of Figure 2. Panels B and C: schemes of tubulin fragments produced by chymotrypsin, similar to Figure 2.

experiment unassembled tubulin was warmed at 37 °C for 30 min in the Mg^{2+}-containing buffer and then taxol was added, the turbidimetric time course of assembly had the same kinetics and reached 90% amplitude of that of the protein aliquot which had taxol from the start. The present proteolysis conditions for the tubulin dimer are the same as previously employed (de la Viña et al., 1988), saving the Mg^{2+} and nucleotide concentrations and the 37 °C preincubation of the samples.

Microtubules were assembled by addition of equimolar taxol to identical aliquots of tubulin, which were processed in parallel with the unassembled samples. Microtubule assembly was monitored by turbidity, sedimentation, and electron microscopy (Figure 1). The tubulin critical concentration was 0.16 ± 0.07 mg mL^{-1}, and no significant assembly was detected without taxol. Therefore, at the 2.0 mg mL^{-1} total concentration employed, 92 ± 3% of the protein was assembled. Taxol-induced microtubules assembled at 37 °C were essentially stable during 20 min at 25 °C, even though they partially depolymerized at 2 °C. The 25 °C polymers observed by electron microscopy with or without 2 mM $CaCl_2$ were microtubules, and the concentration of sedimentable protein was not significantly different from the 37 °C controls. These samples were therefore qualitatively considered as microtubules for the purpose of proteolysis.

Our choice of the taxol-induced microtubules was guided by their stability, by the simple experimental design in direct comparison to identical tubulin samples without taxoid, by the extensive characterization of this system (Andreu et al., 1992, 1994; Díaz & Andreu, 1993; Díaz et al., 1993, 1996), and by the frequent use of taxol to stabilize microtubules in structural studies [for example, Kikkawa et al. (1995)]. We do not think the fact that taxol-induced microtubules have one protofilament less than control microtubules (Andreu et al., 1992) should have any marked influence on their proteolytic accessibility. On the other hand, there is a 0.1 nm increase in tubulin monomer length in the surface lattice of taxol microtubules compared to that of control microtubules, which renders the tubulin to a state similar to the protein liganded to nucleoside triphosphate at the ends of microtubules (Vale et al., 1994; Hyman et al., 1995); the possible effects of this structural change on proteolysis are unknown. At present, we have not detected any changes in the proteolysis patterns of unassembled GDP− and GTP− tubulin (J. M. de Pereda and J. M. Andreu, unpublished). Peptide bonds located on the outer microtubule surface should be similarly sensitive to proteolysis in tubulin dimers and in microtubules. The loss of mobility of tubulin and a possibly restricted diffusion of the protease in the microtubule suspension might be expected to reduce cleavage, but this has not been observed (many cleavages take place to an identical extent within the precision of the blotting methods employed; see below). Note that, given the molecular masses of the proteases employed (Materials and Methods) and the inner diameter of taxol-induced microtubules (Andreu et al.,

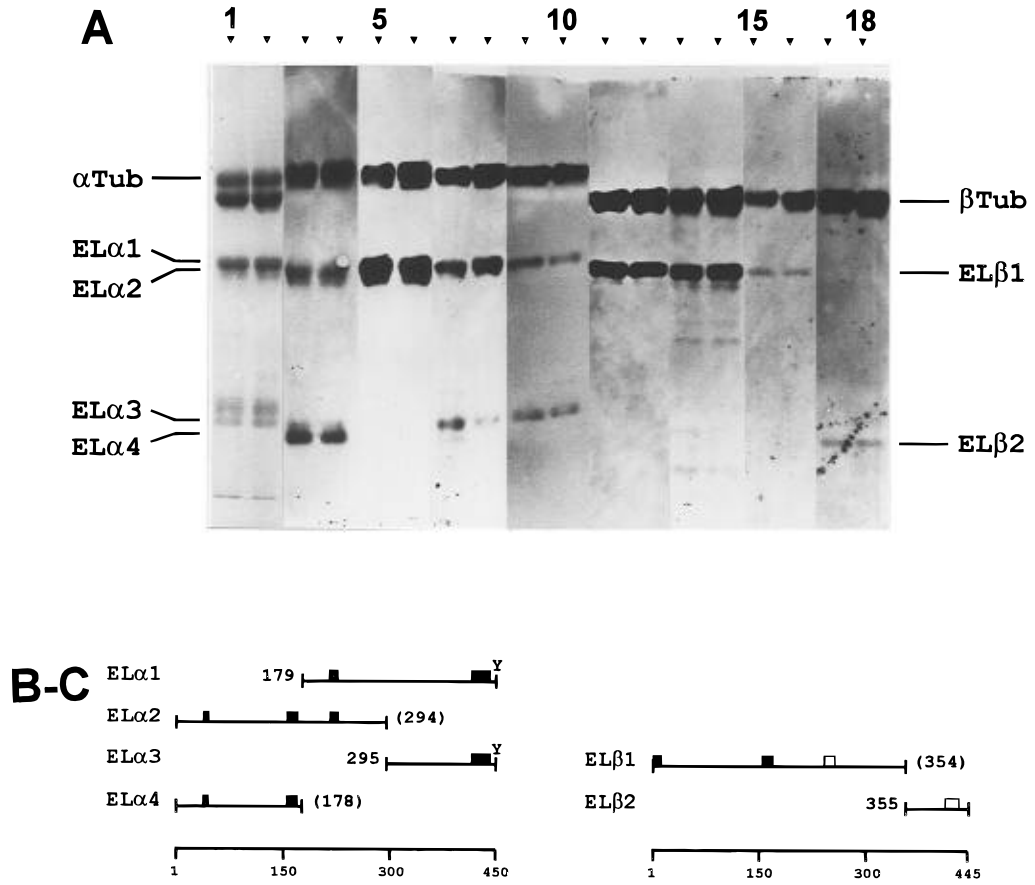

FIGURE 4: Limited proteolysis of tubulin and taxol-induced microtubules by elastase (2% w/w). Panel A contains the immunoblots. Panel B-C shows the schemes of tubulin fragments produced by elastase. These were similar for heterodimeric tubulin and for taxol-induced microtubules (hence there are no separate panels B and C in the figure).

1992), the diffusion of protease molecules into the microtubule lumen and the attack on the inner microtubule surface should be hindered with respect to unassembled tubulin. Any differences observed in the limited proteolysis of both samples should be due to one of the following causes: (a) occlusion of surface bonds of the tubulin dimer by interaction with surrounding tubulin molecules in the microtubule wall or by location in the microtubule lumen, (b) tubulin structural changes induced by assembly and/or taxol binding, or (c) direct occlusion of surface bonds by taxol binding. The latter seems not to be highly probable for this comparatively small ligand, particularly if it does bind in a cleft between protofilaments or elsewhere in the microtubule wall (Andreu et al., 1992, 1994; Díaz et al., 1993; Nogales et al., 1995).

Limited Proteolysis by Trypsin. Native tubulin heterodimers and taxol-induced microtubules were mildly proteolyzed under identical conditions, electrophoresed, and immunoblotted with a panel of sequence-specific antibodies. The protease/tubulin ratio was adjusted to give a fragment pattern as clean as possible while nicking a substantial proportion of tubulin molecules. The results for trypsin are shown in panel A of Figure 2. Panels B and C show the mapping of the tubulin and microtubule fragments onto the sequences of α- and *β*-tubulin with the site-directed antibodies, respectively, as well as their approximate sizes. The fragments included in the analysis are numbered by order of increasing electrophoretic mobility. The results of N-terminal microsequencing of proteolytic fragments of this and the other proteases are collected in Table 1. The main tryptic digestion point is at the Arg339−Ser340 peptide bond of the α-tubulin chain, and it is protected upon microtubule assembly, in agreement with previous results (Brown & Erickson, 1983; Mandelkow et al., 1985; Sackett & Wolff, 1986). Interestingly, a new cleavage point in α-tubulin has been detected, which is only observed in the polymerized state. The small fragment which is generated from microtubules (TRα3, see Figure 2) resisted N-terminal sequencing. From the comparison of its apparent molecular mass with that of the 340−451 fragment sequenced from the dimer, the nicking point should be placed about 12−22 residues upstream of position 339 (note that the apparent molecular masses of the large fragments give larger errors). The only bonds around the zone which are compatible with the cleaving specificity of trypsin are (porcine brain tubulin; Ponstignl et al., 1981) Lys311−Tyr312, Arg320−Gly321, Lys326−Asp327, Lys336−Thr337, and Lys338−Arg339. The latter two are three residues and one residue apart from the bond nicked in the tubulin dimer and would be expected to give a difference in electrophoretic mobility much smaller than observed. Clostripain, which is specific for Arg residues, cleaves the Arg339−Ser340 α-tubulin bond but does not produce a new fragment from microtubules (see below). Therefore, the Lys326−Asp327 bond (followed by Lys311−Tyr312) seems to be the more probable point of preferential taxol microtubule cleavage by trypsin. Trypsin is less active cleaving the *β*-tubulin chain, though two minor cleavage points have been detected. The first is located between residues Lys174 and Val175, and it is exposed in the microtubules. The second should be at a Lys or Arg residue in the zone between residues 250 and 310, and it is protected in microtubules.

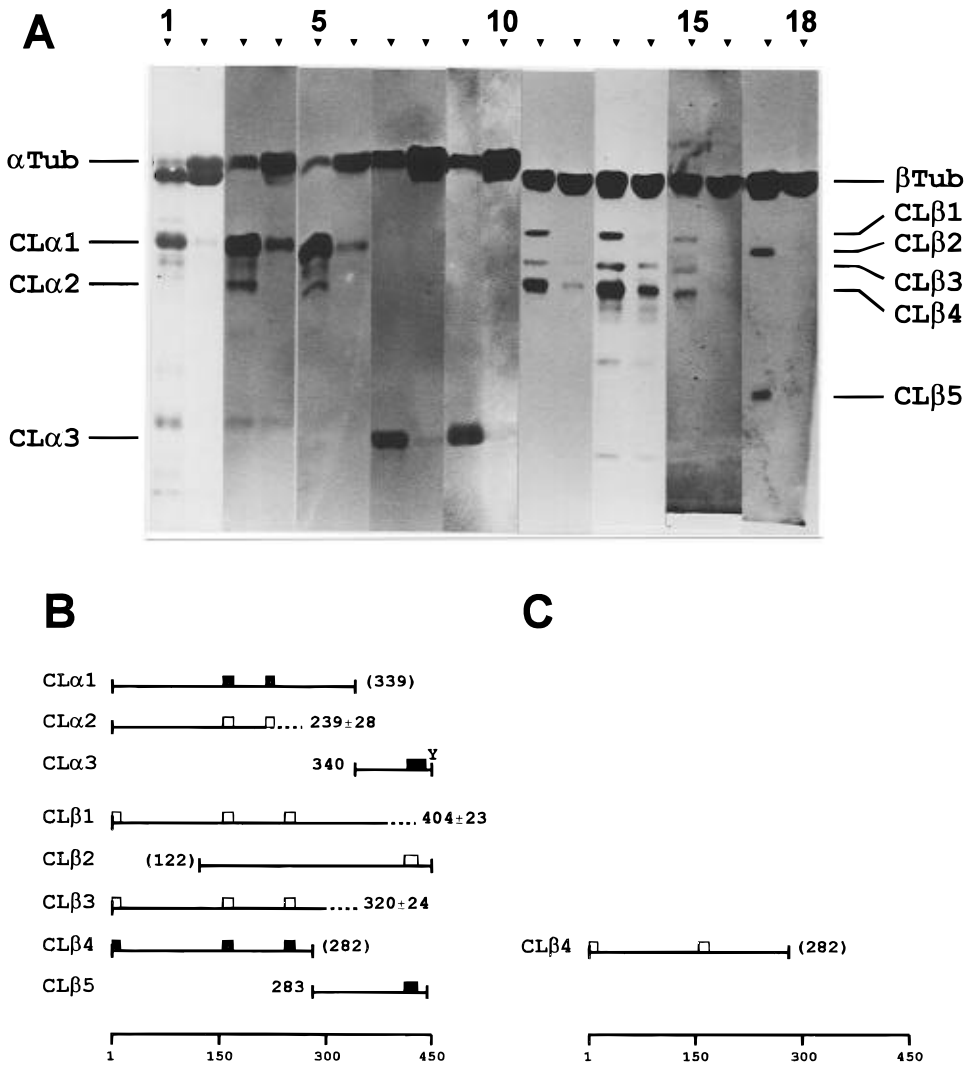

FIGURE 5: Limited proteolysis of tubulin and taxol-induced microtubules by clostripain (2% w/w). Panel A, immunoblots; panels B and C, schemes of tubulin fragments produced by clostripain. The organization of this figure is as in Figure 2.

Limited Proteolysis by Chymotrypsin. The results are shown in Figure 3. Chymotrypsin cleaves the α-tubulin chain at a single point between positions Phe169 and Ser170, which is accessible to proteolysis in microtubules. The main cleavage point is placed in *β*-tubulin at Tyr281−Arg282, and it is protected in microtubules, in agreement with previous results (Brown & Erickson, 1983; Mandelkow et al., 1985; Sackett & Wolff, 1986). There are two other minor nicking points in the *β* chain, which generate the peptides CH*β*3 and CH*β*4, both recognized by the anti*β*(1−13) and anti*β*(153−165) antibodies, though complementary C-terminal peptides have not been detected. On the basis of their apparent molecular masses and the specificity of chymotrypsin, the putative positions of the cleaved bonds are Tyr183−Asn184 and Phe167−Ser168 (although Tyr159 and Tyr200 cannot be totally excluded). These two points are accessible to chymotryptic cleavage in microtubules.

Limited Proteolysis by Elastase. The results shown in Figure 4 and Table 1 indicate that elastase cleaves two peptide bonds in α-tubulin, Ser178−Thr179 and Ala294−Cys295. A minor cleavage point of the *β*-chain is between residues Cys354 and Asp355. These three nicking points are similarly accessible in the tubulin dimer and in microtubules.

Limited Proteolysis by Clostripain. The results are shown in Figure 5. The main cleavage point by clostripain is in the tubulin α chain, between residues Arg339 and Thr340, that is in the same position of trypsin. In contrast with trypsinolysis, a fragment generated from microtubules but not from dimers has not been observed in the clostripain proteolysis. Since clostripain is specific for Arg residues, the putative tryptic digestion of microtubules at position Arg320-Gly321 is improbable. A second, minor cleavage point is located in the region between α-tubulin residues 210 and 265. Both points are protected in microtubules. The *β*-tubulin chain is less sensible to clostripain digestion. Its main cleavage point occurs between Arg282 and Ala283; three other proteolysis points are located in the 125−135, 295−345, and 380−430 zones. From the chemical specificity of clostripain, the first of these has been putatively located at Arg121-Lys122. *β*-Tubulin cleavage by clostripain is practically abolished in microtubules.

Limited Proteolysis by Endoproteinase Lys-C. The results are shown in Figure 6. Controlled proteolysis of heterodimeric α*β*-tubulin with endoproteinase Lys-C occurs preferentially in the α chain, where two main nicking points have been sequenced. One is the Lys40−Thr41 bond, which generates fragment LCα1. This fragment is more abundant in the proteolysis of assembled microtubules, which can be most easily explained by the inhibition of its further cleavage (see below). The side chain of Lys40, which is post-translationally acetylated, is accessible in microtubules to

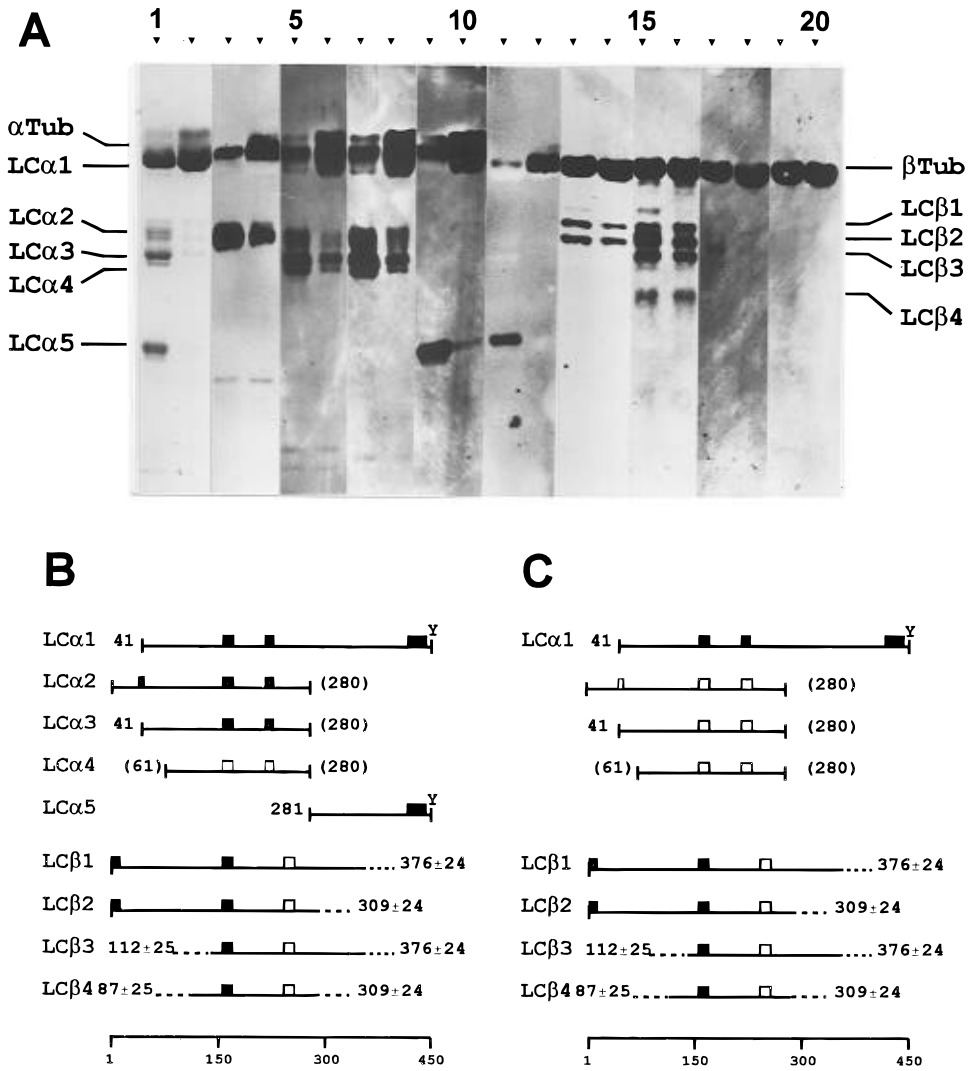

FIGURE 6: Limited proteolysis of tubulin and taxol-induced microtubules by endopeptidase Lys-C (0.5 u/mL). Panel A: lanes 1, 3, 5, 7, 9, 11, 13, 15, 17, and 19, Lys-C-digested heterodimeric tubulin; lanes 2, 4, 6, 8, 10, 12, 14, 16, 18, and 20, Lys-C-digested assembled tubulin. Lanes 1 and 2 are a Coomassie blue-stained gel fragment. Lanes 3−20 are immunoblots with the following site-directed antibodies: 611-B1, lanes 3 and 4; antiα(155−168), lanes 5 and 6; antiα(214−226), lanes 7 and 8; antiα(415−430), lanes 9 and 10; 1A2, lanes 11 and 12; antiβ(1−13), lanes 13 and 14; antiβ(153−165), lanes 15 and 16; antiβ(241−256), lanes 17 and 18; and antiβ(412−431), lanes 19 and 20. Marks on both sides indicate the position of α- and β-tubulin and their fragments. Panels B and C contain schemes of the fragments produced by endoproteinase Lys-C-limited proteolysis of tubulin and taxol-induced microtubules, respectively. The symbols are the same as in Figure 2.

tubulin acetyltransferase (Piperno et al., 1987). The second sequenced nicking point is between residues Lys280 and Ala281, and in contrast to the first one, it is protected upon assembly. This is similar to the main chymotrypsin nicking point Tyr281-Arg282 in the β chain, which is also protected in microtubules. A third, minor cleavage point in α-tubulin is placed downstream from Lys40 and before epitope α(155−168), and it is also occluded in microtubules. The Lys residues in this region are (porcine brain α-tubulin) Lys60, Lys95, Lys110, and Lys122 (Ponstingl et al., 1981). On the basis of the apparent molecular masses of the LCα3 and LCα4 fragments, the more probable position of this cleavage point is Lys60−His61. Note that the Lys40−Thr41 and Lys280−Ala281 bonds are not digested by trypsin, although they satisfy its chemical specificity. Although the endopeptidase Lys-C digestion of β-tubulin is very limited, a minimum of three cleavage points have been detected in the 60−140, 285−330, and 350−400 zones. These three points are also cleaved in assembled tubulin. The porcine brain β-tubulin sequence contains the Lys58, Lys103, Lys122, and Lys154 residues (Krauhs et al., 1981) around the 60−140 zone.

Limited Proteolysis by Thermolysin. As shown by Figure 7, the α-tubulin peptide map produced by controlled digestion with thermolysin, a low-specificity protease, indicates the presence of three major significant nicking points. From the sequencing of fragment THα1, one of these is between residues Thr41 and Ile42, in agreement with the results of Paschal et al. (1989). This point is next to the Lys40−Thr41 bond which is cleaved by endoproteinase Lys-C (see above). The amount of THα1 generated from microtubules is larger than that from tubulin dimers, suggesting not only accessibility (Brown & Erickson, 1983) but enhanced local sensitivity to thermolysin in the assembled state. A second digestion point is located in the 170−190 zone, and a third cleavage zone is around position 300. Both of them are not significantly modified in microtubules. Thermolysin digestion of β-tubulin yields a complex set of fragments. We have interpreted that cleavages occur in two zones of the sequence. On the basis of the antigenic reactivity and

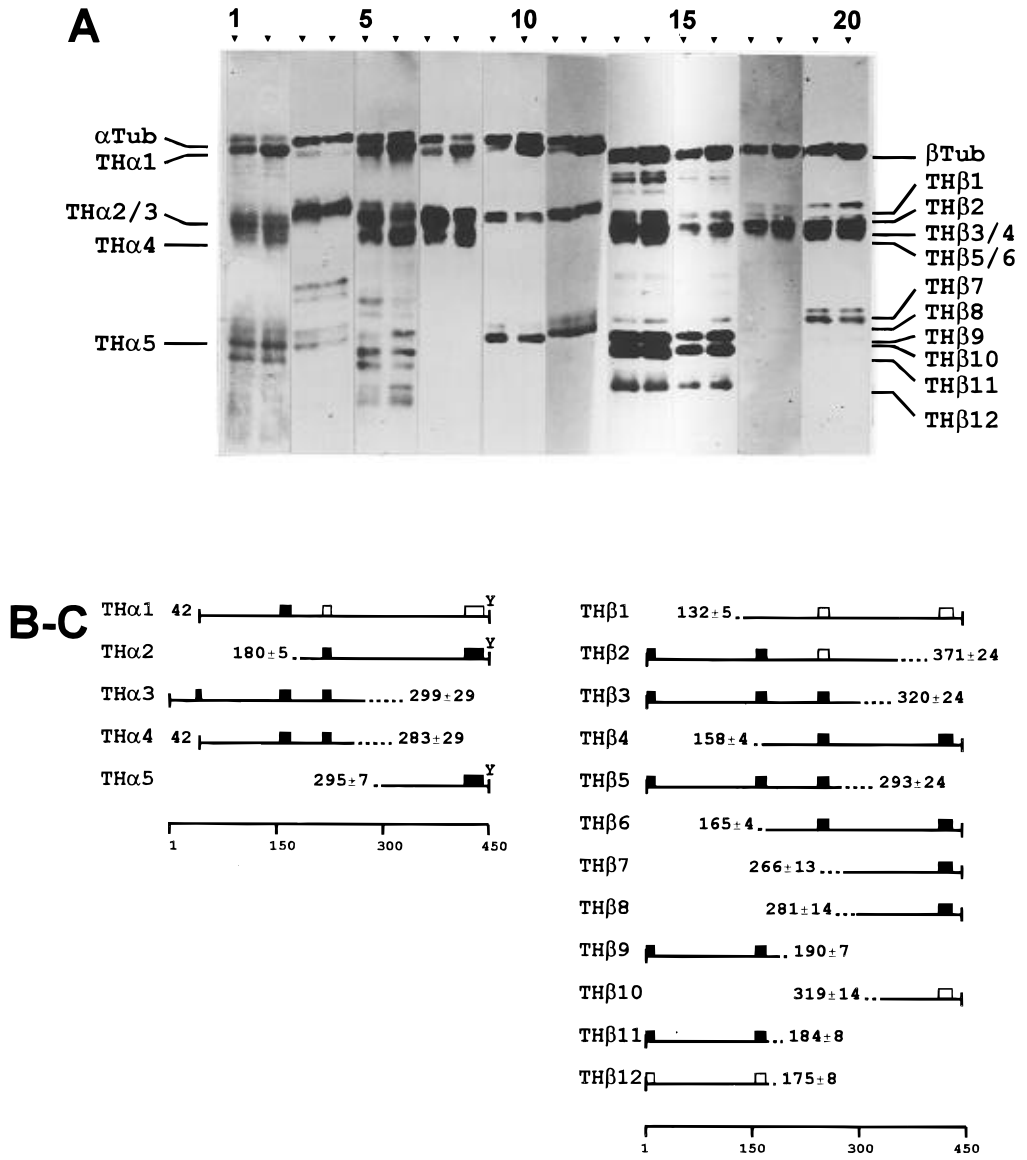

FIGURE 7: Limited proteolysis of tubulin and taxol-induced microtubules by thermolysin (1.5% w/w). Panel A contains the immunoblots in the same order as Figure 6 and panel B-C the schemes of tubulin fragments produced by thermolysin (similar to Figure 4). Fragment THα1 is obtained in larger amounts from dimers than from microtubules. The rest of the thermolysin fragments analyzed show no difference. Note that the reaction of fragment THβ10 with the antiβ(412−431) antibody is very faint and hardly reproduces in pictures.

complementary apparent sizes of the different fragments, the first of these zones should be located closely downstream from epitope β(153−165) and includes three nicking points. The second zone includes another three nicking points situated roughly between residues 275 and 350. The β-tubulin thermolytic patterns are essentially identical in tubulin dimers and microtubules.

Limited Proteolysis by Protease V8. The results are shown in Figure 8. Protease V8 cleaves α-tubulin at four points in its sequence. A major nicking point is between residues Glu168 and Phe169, next to the chymotrypsin nicking point Phe169-Ser170. Closely downstream there is a minor nicking point whose putative localization, based on V8 specificity, is Glu183−Pro184. The fragment 184−451 (complementary to 1−183, V8α6) has not been detected, but it could be masked by the major fragment 169−451 (V8α1), as they both would be recognized by the same antibodies used and their difference in molecular mass falls within experimental error. A third cleavage point has been determined between residues Glu290 and Ile291. The cleavage of these three internal positions is not very different in tubulin dimers and microtubules. Protease V8 also attacks the carboxy-terminal region of the α-tubulin, since fragments are produced which are recognized by the antiα(415−443) antibody but not by the 1A2 antibody, which recognizes the tyrosilated intact carboxy end of the α-tubulin chain. This nicking point is probably located within the last 15 residues. A small but significant increase of the presence of fragments detected by the 1A2 antibody has been observed in the digestion of microtubules, suggesting that the carboxy-terminal nicking point becomes partially protected upon assembly. Protease V8 attacks the β-tubulin predominantly at its carboxy-terminal region. The positions of three nicking points have been estimated on the basis of the reactivity of the fragments with the antiβ(412−431) monospecific antibody and their apparent size. These positions are putatively located before, within, and after the β(412−431) sequence. Note that in β-tubulin protease V8 nicking points in this zone include more inner positions than that in α-tubulin. In addition, an internal cleavage point has been detected, near residue 320. From the specificity of the protease, the possible position of this nicking point would be one of the following bonds: Asp295−Ala296, Asp304−Pro305, Glu325−Val326, or Glu328−Gln329. The sensitivity of

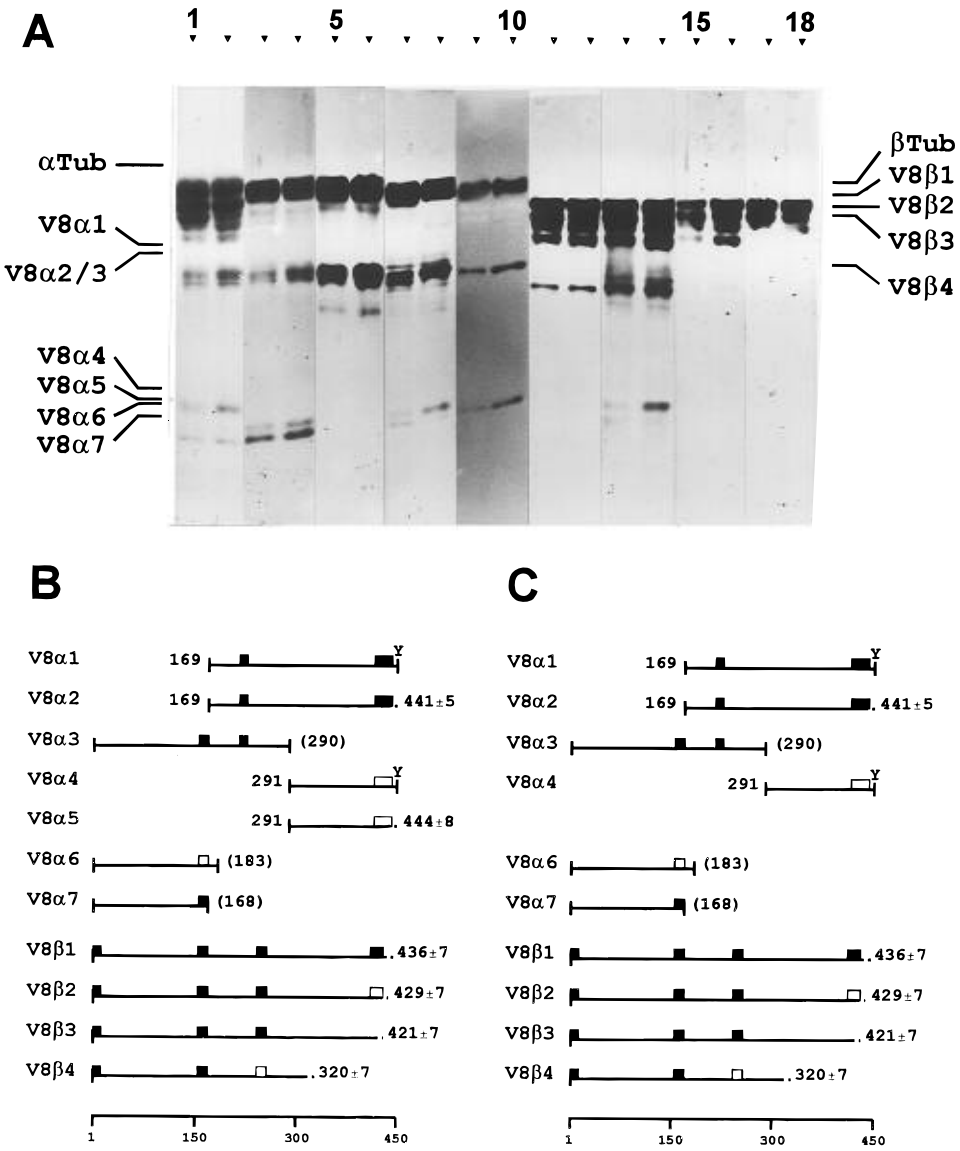

FIGURE 8: Limited proteolysis of tubulin and taxol-induced microtubules by protease V8 (2% w/w). Panel A contains the immunoblots, in the same order as in Figure 2, and panels B and C contain the schemes of tubulin fragments produced by the protease V8.

β-tubulin to protease V8 attack is similar in microtubules to that of the dimer state.

Proteolysis by Papain. Limited cleavage of α-tubulin by papain occurs in three main positions, as shown in Figure 9. The major internal point is at the Ser178−Thr179 bond. This is coincident with one elastase nicking point (see above). A minor cleavage point has been observed in the 305−365 region. These two internal positions have a similar sensibility to proteolysis in tubulin dimers and in microtubules. The third digestion point is at the carboxy-terminal zone. Antibody 1A2 recognizes practically no band in the immunoblots of digested dimeric tubulin, indicating a marked proteolytic sensitivity of the C-terminal tyrosine. However, the proteolysis at this region does not produce any significant shift in the apparent molecular mass of the fragments, suggesting that cleavage is limited to the very last positions in the sequence. In contrast, the same antibody reacts strongly with the α chain and with its fragment PAα3 when microtubules are digested, indicating that the extreme carboxy terminus of α-tubulin is protected upon microtubule assembly. The pattern of proteolysis of β-tubulin by papain is complex and has been interpreted as taking place in two internal regions and at the carboxy-terminal zone. Three cleavage points have been detected in the 170−195 zone, shortly downstream from epitope β(153−165), and two proteolytic attack points in the 270−310 region. These appear similarly exposed in tubulin dimers and in microtubules. However, the papain proteolysis of assembled tubulin generates new β-tubulin fragments which are not even detected from the tubulin dimer. Most prominent is PAβ1, which comes from the removal of several C-terminal residues. The fragment PAβ6 is produced by a new cleavage around position 265. Fragment PAβ5 and the new doublet PAβ9−PAβ11 may be explained by the C-terminal cleavage of the corresponding fragments PAβ4, PAβ7, and PAβ8, which should be generated in more abundance from microtubules than from the tubulin dimer [see the blot with the antiβ(412−431) antibody in lanes 19 and 20 of Figure 9]. These papain fragments of microtubules may either appear as a result of conformational changes or pass undetected in dimers due to more extensive secondary cleavages by this nonspecific protease.

Limited Proteolysis by Subtilisin. As shown in Figure 10, the main internal point of α-tubulin digestion by subtilisin is placed between residues Ala180 and Val181. A second minor digestion point occurs near that position, probably

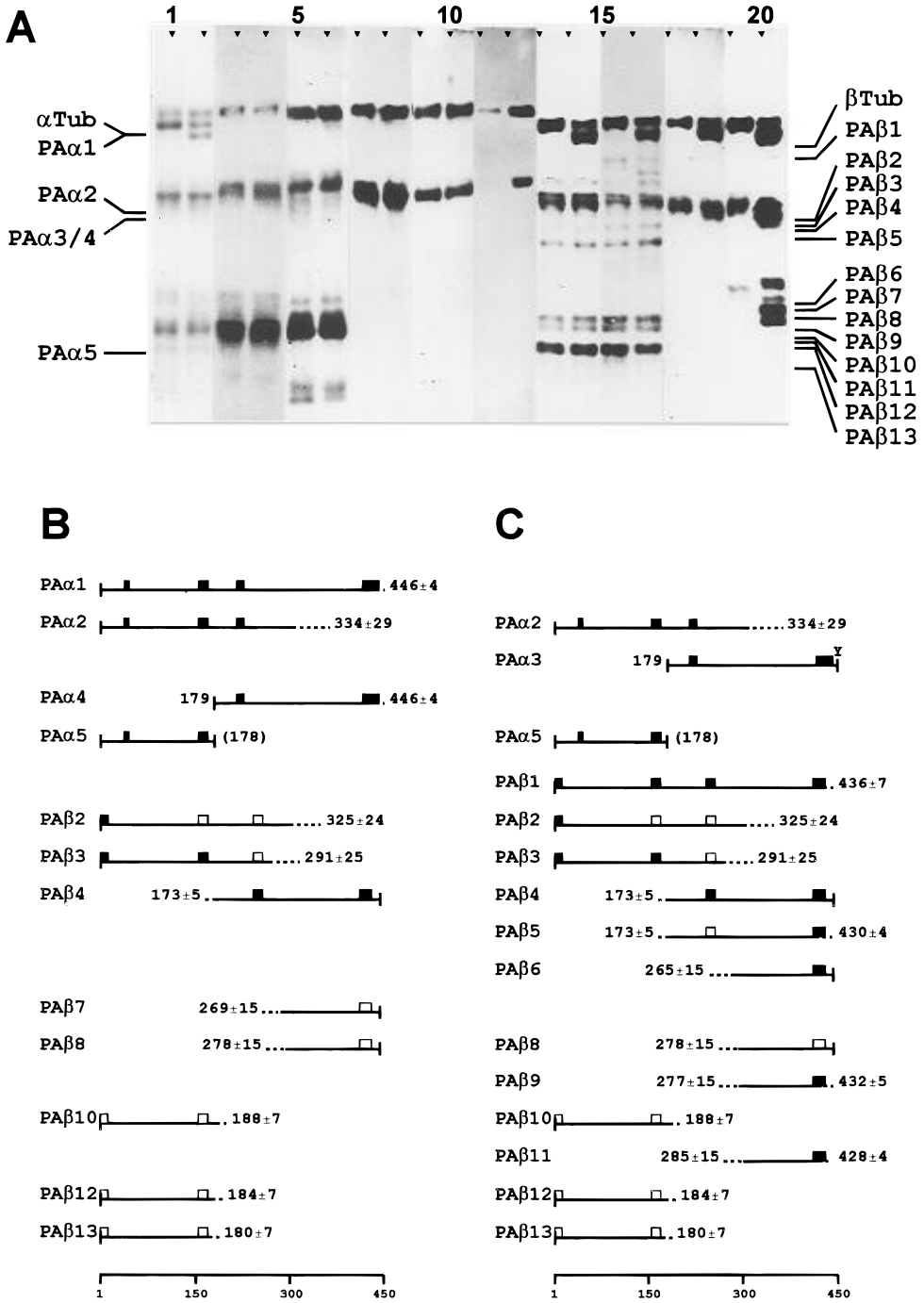

FIGURE 9: Limited proteolysis of tubulin and taxol-induced microtubules by papain (1% w/w). Panel A, immunoblots, in the same order as in Figure 6; panels B and C, schemes of tubulin fragments produced by papain.

downstream in the sequence. Another two internal cleavage points have been detected in the 285−325 region. Carboxy-terminal cleavage generates fragments which are recognized by immunoblot with an antiα(415−443) antibody but not with the 1A2 antibody. This suggests that the single nicking point detected is placed within the last residues of the sequence. On the basis of the reactivity with an antiα(430−443) antibody under very similar conditions, the cleavage point has been mapped near the Glu441-Gly442 residues (M. A. Arévalo and J. M. Andreu, unpublished results). Redecker et al. (1992) have identified the Asp438−Ser439 bond as the major cleavage point by subtilisin in porcine brain α-tubulin. Subtilisin digestion at the carboxy-terminal zones of tubulin is known to depend strongly on solution conditions, including the buffer and the presence of millimolar concentrations of divalent cations (Lobert et al., 1993). The only significant difference observed in the controlled digestion by subtilisin of α-tubulin in microtubules is an increase in the intensity of the bands recognized by the 1A2 antibody, which indicates a protection of its extreme carboxy terminus upon assembly. Note that tubulin tyrosine ligase works preferentially on nonassembled tubulin (Thompson, 1982; Wheland & Weber, 1987); however, tubulin tyrosine carboxypeptidase is more efficient on microtubules (Kumar & Flavin, 1981). Subtilisin digests the β-tubulin chain at three internal zones and at the carboxy-terminal region. On the basis of the immunoreactivity of the fragments, the first internal proteolysis zone is closely downstream from epitope β(153−165) and consists of three nicking sites. The two other internal cleavage points occur around positions 281 and 319−354; the latter appears protected in the limited proteolysis of microtubules (see fragment SBβ10). Three

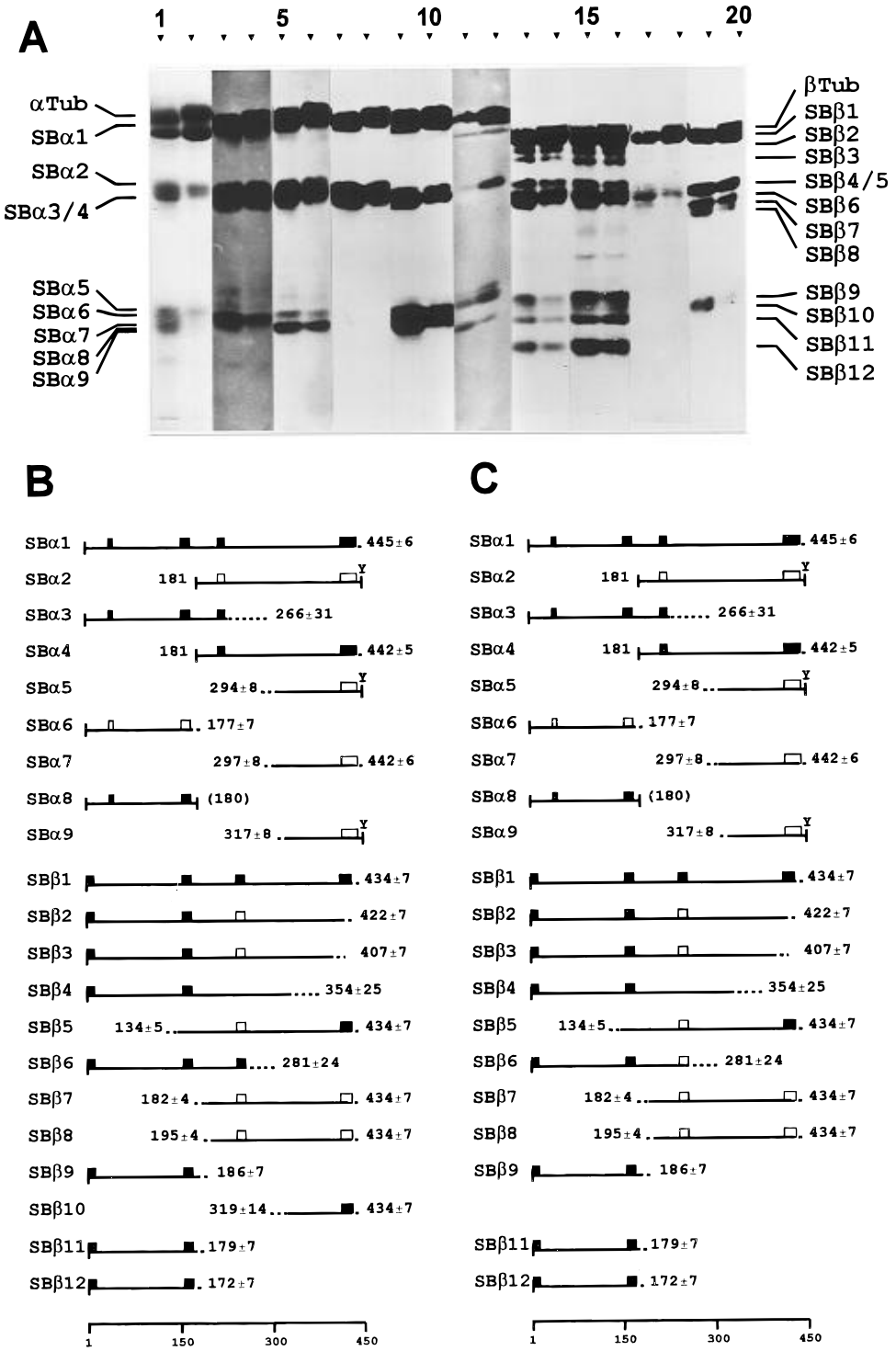

FIGURE 10: Limited proteolysis of tubulin and taxol-induced microtubules by subtilisin (0.7% w/w). Panel A contains the immunoblots in the same order as in Figure 6, and panels B and C contain the schemes of tubulin fragments produced by subtilisin.

cleavage points have been observed at the carboxy-terminal zone. The major cleavage does not abolish immunoreactivity with the antiβ(412−431) antibody, and its apparent location is around residue 434. The two other minor points of subtilisin digestion observed in this work are located around positions 407 and 422. From the difference spectroscopical titration of the tyrosine residues lost by subtilisin digestion, proteolysis should occur near positions Glu421-Tyr422 and Asp431-Glu432 (M. A. Arévalo and J. M. Andreu, unpublished results). Redecker et al. (1992) have identified the Gln433-Gly434 residues as the main subtilisin cleavage point of porcine brain β-tubulin, as well as a minor cleavage point at the His396−Trp397 bond. Limited subtilisin proteolysis of a model carboxy-terminal peptide of β-tubulin has permitted the sequencing of main fragments corresponding to cleavage of bonds 397−398, 409−410, and 422−423 (J. Evangelio and J. M. Andreu, unpublished). The above comparisons strongly suggests that the three carboxy-terminal cleavages of β-tubulin by subtilisin detected in the present study are located at positions 409−410, 422−423, and 433−434, with a maximal uncertainty of plus or minus three residues. No significant change in the sensitivity of the β-tubulin carboxy-terminal region to subtilisin is evident upon assembly in microtubules. However, there is an increase in the intact β chain in microtubules, which might indicate a protection of the main cleavage point 433−434

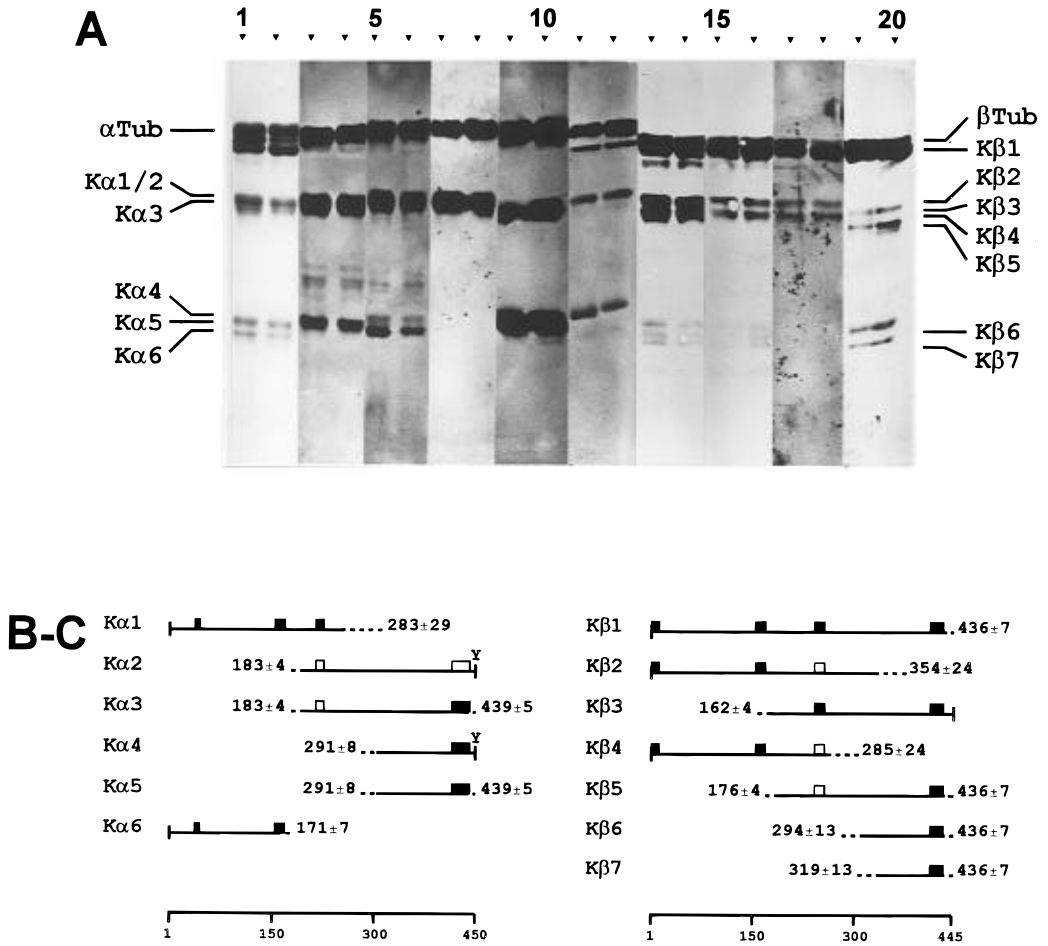

FIGURE 11: Limited proteolysis of tubulin and taxol-induced microtubules by the proteinase K (0.1% w/w). Panel A, immunoblots, in the same order as in Figure 6; panel B-C, scheme of tubulin fragments produced by the proteinase K (these were similar for heterodimeric tubulin and taxol-induced microtubules; hence, there is no separate panel C)

or more probably of the internal cleavage in the zone between positions 310 and 355. It has been reported that a β-tubulin bond around position 435 becomes more accessible in taxol-induced microtubules (Lobert & Correia, 1992).

Limited Proteolysis by Proteinase K. These results are shown in Figure 11. Proteinase K cleaves α-tubulin in two internal positions of the sequence, approximately in the 165−190 and 280−300 zones, and there is a third nicking point in the carboxy-terminal region. Cleavage of this region does not affect the immunoreactivity with antiα(415−443) antibodies, but it eliminates reactivity with the 1A2 antibody, indicating that the proteolytic attack is limited to the last 10−20 residues of the sequence. In β-tubulin, three internal nicking points have been detected. One is most probably localized in the 160−180 zone and the two other in the 285−345 zone. Proteinase K also cleaves the carboxy-terminal zone of β-tubulin, but it does not abolish immunoreactivity with the antiβ(412−431) antibody. On the basis of this and the preferred chemical specificity of proteinase K (an aliphatic or aromatic residue in the carboxy side of the peptide bond hydrolyzed), this cleavage site should be located within the segment Tyr422−Phe436. The limited proteolysis points of proteinase K on both α- and β-tubulin are accessible in microtubules.

Limited Proteolysis by Endoproteinase Asp-N. As shown in Figure 12, a single majority nicking point of β-tubulin by endoproteinase Asp-N has been detected. It is located in the carboxy-terminal zone and is exposed in microtubules. From the reactivity of the fragment with the antiβ(412−431) antibody and the specificity of this endoproteinase, the possible positions for the major β2 brain isoform are Gln426−Asp427 or Ala430−Asp431. Redecker et al. (1994) have described the cleavage of axonemal β-tubulin from *Paramecium* (which has no equivalent for the mammalian Asp431) at the Gln425−Asp426 bond. Endoproteinase Asp-N cleaves α-tubulin insignificantly under the mild conditions assayed. This protease may constitute a good tool for specifically cleaving the C terminus of β-tubulin.

Limited Proteolysis by Bromelain. Bromelain digests α-tubulin in six points of its sequence, as indicated by the results shown in Figure 13. Two points of proteolytic attack have been detected in positions shortly downstream from epitope α(155−168). Another three nicking points are placed around positions 256, 334, and 372. The presence of a cleavage point in the carboxy-terminal region has also been observed, which abolishes immunoreactivity with the 1A2 antibody (not shown) and reduces the reactivity with the antiα(415−443) antibodies. Therefore, it is probably located within the last 20 residues. There is no significant change in the limited proteolysis of α-tubulin by bromelain when it is assembled into microtubules. In the limited proteolysis of β-tubulin by bromelain, four main nicking points have been observed. The positions of the two internal points have been determined by N-terminal microsequencing of the fragments and are Gly93-Gln94 and Gly277-Ser278. These two internal positions are sensitive to limited proteolysis in the microtubules as well. The other two points of proteolysis attack are at the carboxy-terminal region. Large

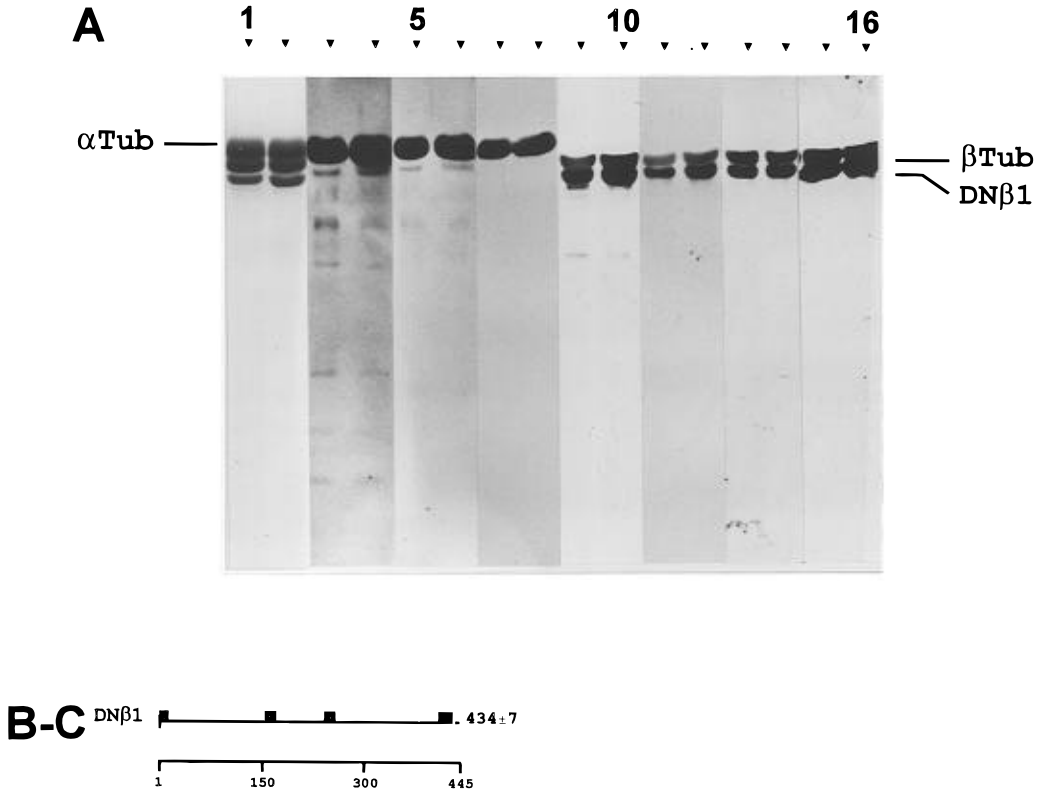

FIGURE 12: Limited proteolysis of tubulin and taxol-induced microtubules by endoproteinase Asp-N (0.06% w/w). Panel A: lanes 1, 3, 5, 7, 9, 11, 13, and 15, endoproteinase Asp-N-digested heterodimeric tubulin; lanes 2, 4, 6, 8, 10, 12, 14, and 16, endoproteinase Asp-N-digested assembled tubulin; Lanes 1 and 2 are a Coomassie blue-stained gel fragment. Lanes 3−16 are immunoblots with the following site-directed antibodies: antiα(155−168), lanes 3 and 4; antiα(214−226), lanes 5 and 6; antiα(415−430), lanes 7 and 8; antiβ(1−13), lanes 9 and 10; antiβ(153−165), lanes 11 and 12; antiβ(241−256), lanes 13 and 14; and antiβ(412−431), lanes 15 and 16. Marks on both sides indicate the position of α- and β-tubulin and the fragment. Panel B-C: scheme of the majority fragment similarly produced by Asp-N proteinase-limited proteolysis of heterodimeric tubulin or taxol-induced microtubules.

and small fragments digested in these positions are recognized by antiβ(412−431) antibodies, suggesting that digestion is limited to the last 15 or 20 residues of the β-tubulin sequence. The fragments BRβ5 and BRβ6 recognized by the antiβ(412−431) antibody are not detected in microtubule proteolysis. Parallel to this, an increase is observed in the intensity of the next band recognized by this antibody, BRβ7, suggesting an enhancement of the inner C-terminal cleavage in microtubules.

CONCLUSIONS

In this study, we have systematically used limited proteolysis to nick and map surface zones of native tubulin in its unassembled and assembled states. Figure 14 and Table 2 summarize the results of limited proteolysis of $\alpha\beta$-tubulin dimers and taxol-induced microtubules with a panel of 12 proteases of different specificities. A total of 133 proteolytic fragments (see Figures 2−13) have been located on the tubulin sequences with the aid of site-directed antibodies. This, complemented with critical use of the fragment apparent molecular sizes, has permitted the mapping of the approximate position of 80 surface cleavage points. Of these, 18 protease cleavage points have been exactly determined by sequencing their N-terminal fragments and 6 have been deduced from the specificity of the protease (Figure 14, Table 2). In addition, sequences recognized by the site-directed antibodies (indicated by the rectangles, Ac and Y in Figure 14) are generally accessible at the surface of tubulin. The possibility that some of the nick sites may be secondary nonsurface sites made accessible by other initial cleavages is particularly unlikely for the more specific proteases and also for the clusters of nick sites accessible to several different proteases.

Proteolytic nicking points are not distributed randomly along the tubulin sequences but cluster in five zones, labeled A−E in Figure 14. This map does not exclude other possible proteolysis sites. Actually, it is an extension of our earlier maps (de la Viña et al., 1988; Andreu & Arévalo, 1993). The proteolysis zones are in equivalent positions in both α and β sequences, with the exception of zone A. From the positions of sequenced nicking points, the internal proteolysis zones extend to maximum lengths of 12−18 residues (zone B) and 7−15 residues (zone C), which suggests that each zone may correspond to one or more surface structural elements having low structural rigidity, such as surface loops.

From 80 nicking points, 60 are similarly accessible on the surface of microtubules and tubulin dimers (labeled S in Figure 14), while 14 are protected in microtubules (marked P in the figure) and 4 are cleaved in microtubules but not in dimers (labeled M in the figure). The surface bonds identified as exposed or occluded in taxol-induced microtubules are listed in Table 2. Surface sequences of the tubulin dimer which have been reported to be exposed or occluded from their specific antibodies in microtubules (Arévalo et al., 1990) are marked E and O, respectively, in Figure 14. The proteolytic susceptibility of tubulin sequences in taxol-induced microtubules may be modified for several reasons (see Results and Discussion). Each limited proteolysis zone is discussed in detail elsewhere (de Pereda et al., 1996). A brief summary of zones A−D is as follows.

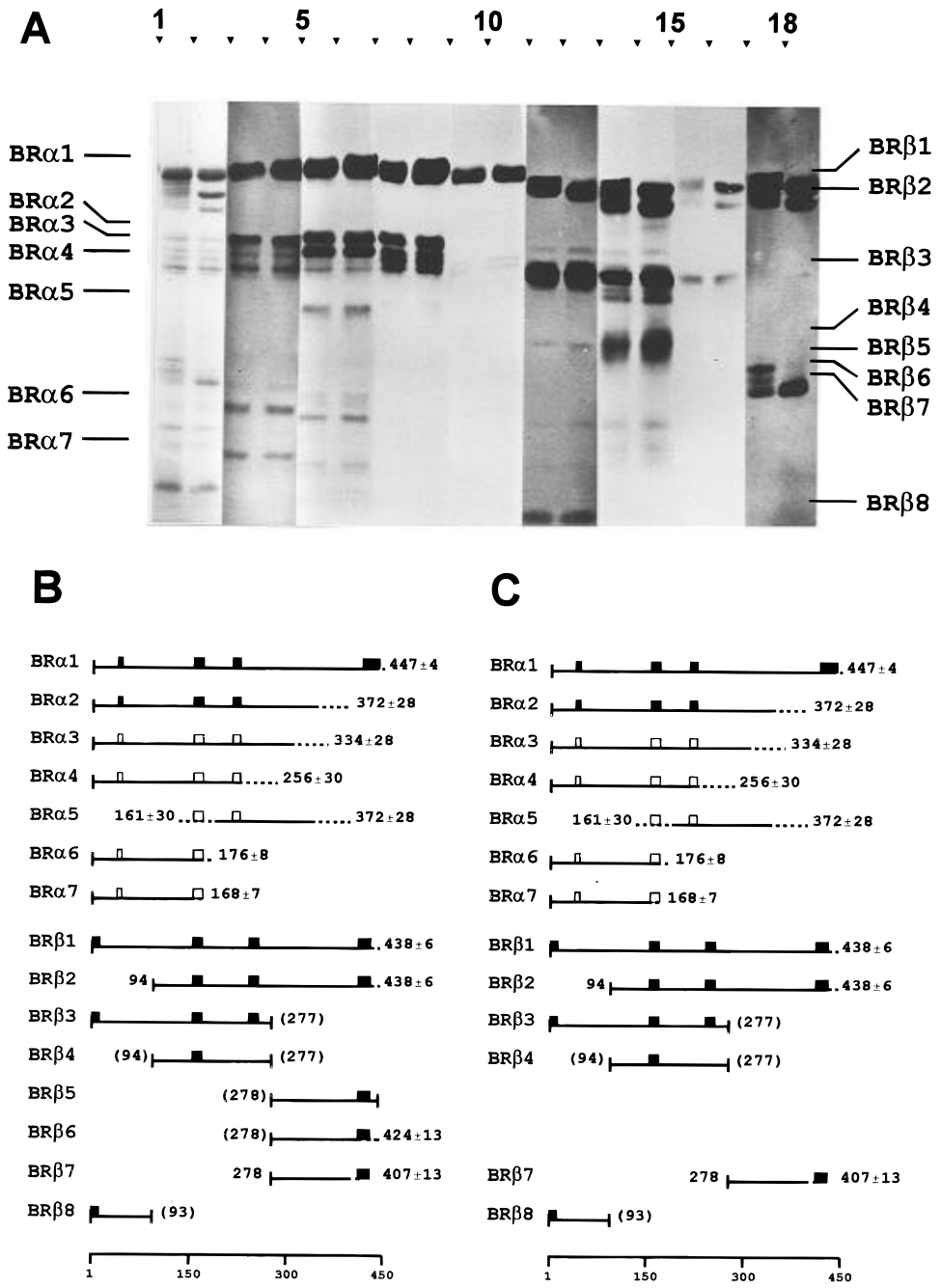

FIGURE 13: Limited proteolysis of tubulin and taxol-induced microtubules by bromelain (5% w/w). Panel A contains immunoblots in the same order as in Figure 2. The antityrosilated α-tubulin antibody 1A2 reacted with none of the bromelain fragments (data not shown). Panels B and C are the schemes of the tubulin fragments.

Proteolysis zone A is exposed in microtubules, in agreement with the accessibility of acetyl-Lys40. Proteolysis zone B is exposed in both subunits, although the immediate sequence α(155−168) is not immunoreactive in microtubules and has been tentatively located at large surface grooves (Arévalo et al., 1990). Zone C shows protection around residue 280 (except for bromelain cleavage of β-tubulin) and exposure of α-tubulin residues 290−295. This is suggestive of the location of this zone at large microtubule surface grooves. In proteolysis zone D, the α-tubulin bond Arg339−Ser340 is characteristically protected from cleavage by trypsin and clostripain in microtubules. This tryptic cleavage jumps back in microtubules to a nearby position (probably 326−327 or 311−312), suggesting a structural change. The β-tubulin bond Cys354−Asp355 remains accessible to the attack of elastase in microtubules. Cys354 is known to be less than 0.9 nm from Cys239 (Little & Ludueña, 1985). Zone E, the carboxy termini of both chains, which is the main site of post-translational modifications and is considered to be in general accessible to antibodies and proteases in assembled microtubules, shows interesting effects. The last residues of the α-tubulin chain, ending in the C-terminal tyrosine, are comparatively protected in microtubules against cleavage by subtilisin, papain, and protease V8. In contrast, the carboxy terminus of β-tubulin remains accessible to multiple cleavage by five proteases in microtubules. Moreover, it exhibits two cleavages by papain which are not observed in the unassembled tubulin dimer. The fact that in general terms the C terminus of α-tubulin becomes comparatively protected by assembly, while the C terminus of β-tubulin remains exposed, has clear topological implications. It suggests that the former is near one end of the heterodimer in the microtubule protofilament, while the latter is near the intersubunit interface. This is compatible with the reported

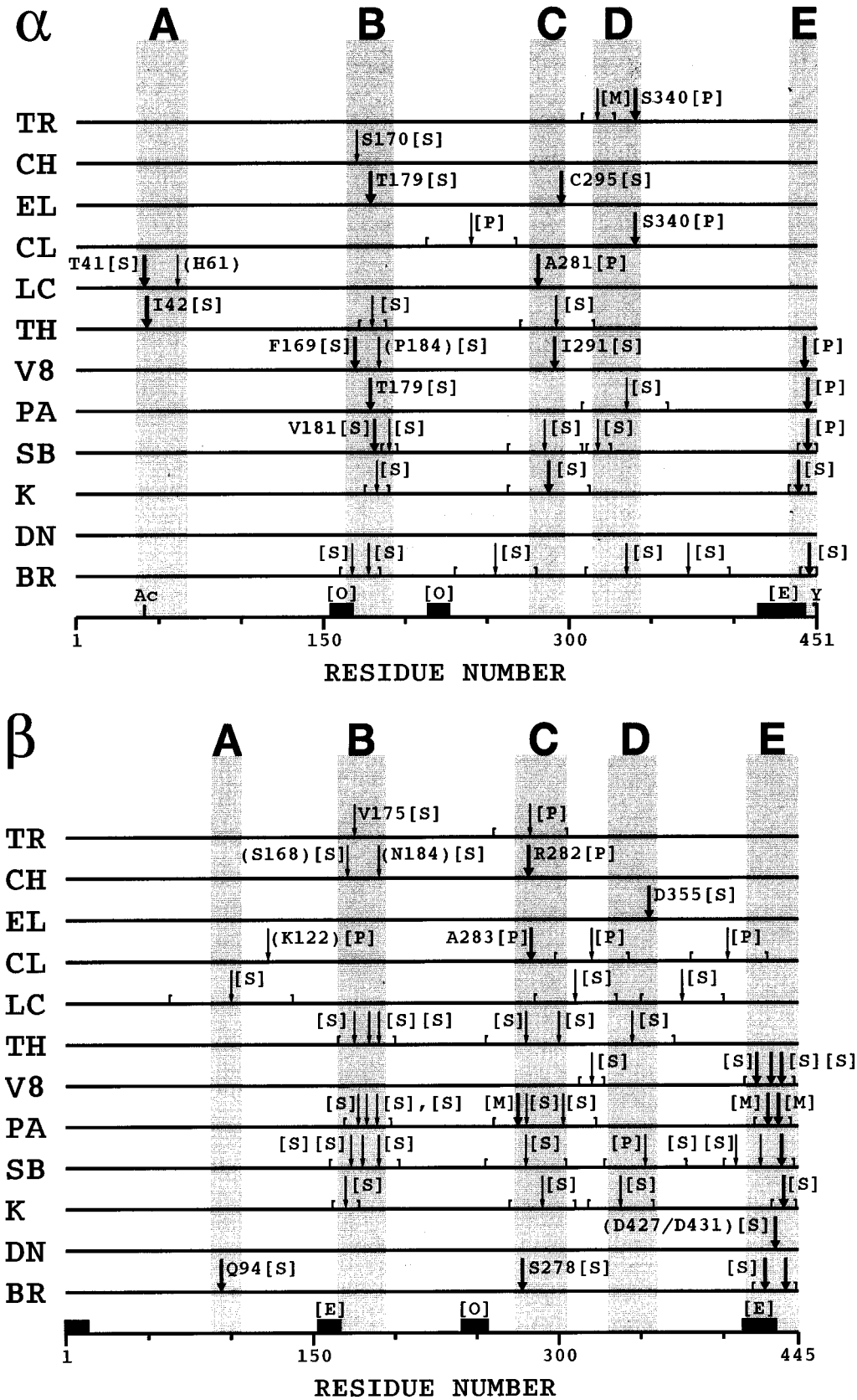

FIGURE 14: Maps of the limited proteolysis of α- and *β*-tubulin by 12 proteases, which summarize the position of the nicking points. The position of proteolyitc sites determined by N-terminal microsequencing of fragments is indicated by the single-letter code and number of the first residue after it; residues in parentheses are putatively assigned positions. The positions of the rest of the cleavage points were determined from the antibody reactivity of the fragments and its corrected apparent molecular mass, and the estimated errors are indicated. Major and minor cleavage sites are indicated by heavy and light tracing arrows, respectively. Shaded areas mark the approximate extension of the five preferential cleavage regions. The comparative sensitivity of the cleavage points upon taxol-induced microtubule assembly is indicated between brackets: [S] indicates surface sites exposed in the tubulin $\alpha\beta$ dimer and microtubules, while [P] indicates sites which are protected in the polymer form, and [M] indicates sites which were detected exclusively in microtubules. The sequences recognized by the site-directed antibodies employed to analyze the peptide maps are indicated by the solid rectangles, and the symbols Ac and Y; the reported accessibility of these sequences in microtubules is indicated by the letters [E], exposed, and [O], occluded [see Arévalo et al. (1990), Piperno et al. (1987), Wheland et al. (1983), and Gundersen et al. (1984)].

Table 2: Exposure of α*β*-Tubulin Dimer Surface Residues in Taxol-Induced Microtubules

tubulin subunit	residues	exposure in microtubules[b]
α	Lys40-Thr41-Ile42	S
	Glu168-Phe169-Ser170	S
	Ser178-Thr179-Ala180-Val181	S
	(Glu183-Pro184)[a]	S
	Lys280-Ala281	P
	Glu290-Ile291	S
	Ala294-Cys295	S
	Arg339-Ser340	P
β	Gly93-Gln94	S
	(Arg121-Lys122)[a]	P
	(Phe167-Ser168)[a]	S
	Lys174-Val175	S
	(Tyr183-Asn184)[a]	S
	Gly277-Ser278	S
	Tyr281-Arg282-Ala283	P
	Cys354-Asp355	S
	(Glu426-Asp427) or (Ala430-Asp431)[a]	S

[a] Residues putatively identified from protease specificity and apparent size are in parentheses. [b] Surface-exposed (S) and occluded (P) (protected from protease attack). The exposure of α-tubulin (Lys60-His61) in microtubules was not determined.

increase in proteolytic accessibility of *β*-tubulin to carboxy-terminal cleavage by subtilisin under heterodimer dissociation conditions (Sackett et al., 1989) and supports the models proposed by Kirchner and Mandelkow (1985) and Ward et al. (1994).

The unequivocal surface positioning of protease nicking points reported in this work may be employed as a set of constraints for any emerging three-dimensional structure of tubulin from X-ray or electron crystallography [for example, see Nogales et al. (1995)]. Once the atomic structure of tubulin is known, it will be employed to model high-resolution structures of microtubules fitting cryoelectron microscopy and X-ray fiber diffraction data; the identification of residues at the microtubule surface should help to unambiguosly orient the tubulin molecules in the microtubule lattice. The use of the limited proteolysis and other biochemical data in combination with secondary structure analysis of tubulin and the bacterial cell division protein FtsZ is demonstrated in the following paper (de Pereda et al., 1996).

ACKNOWLEDGMENT

We thank Javier Varela for microsequencing, Juan Evangelio for sedimentation velocity, and Dr. Isabel Barasoain for the monoclonal antibody to *β*(1−13) tubulin.

SUPPORTING INFORMATION AVAILABLE

Table showing the characteristics of tubulin proteolytic fragments and a figure showing the plots of the apparent versus theoretical M_r values of tubulin fragments (7 pages). Ordering information is given on any current masthead page.

REFERENCES

Alexander, J. E., Hunt, D. F., Lee, M. K., Shabanowitz, J., Michel, H., Berlin, S. C., Macdonald, T. L., Sundberg, R. J., Rebhun, L. I., & Frankfurter, A. (1991) *Proc. Natl. Acad. Sci. U.S.A. 88*, 4685−4689.

Amos, L. A., & Klug, A. (1974) *J. Cell Sci. 14*, 523−549.

Andreu, D., de la Viña, S., & Andreu, J. M. (1988) *Int. J. Pept. Protein Res. 31*, 555−566.

Andreu, J. M., & Muñoz, J. A. (1986) *Biochemistry 25*, 5220−5330.

Andreu, J. M., & Arévalo, M. A. (1993) *Cell. Pharmacol. 1*, s11−s16.

Andreu, J. M., & de Pereda, J. M. (1993) *Cell Motil. Cytoskeleton 26*, 1−6.

Andreu, J. M., Gorbunoff, M. J., Lee, J. C., & Timasheff, S. N. (1984) *Biochemistry 23*, 1742−1752.

Andreu, J. M., Bordas, J., Díaz, J. F., García de Ancos, J., Gil, R., Medrano, F. J., Nogales, E., Pantos, E., & Towns-Andrews, E. (1992) *J. Mol. Biol. 226*, 169−184.

Andreu, J. M., Díaz, J. F., Gil, R., de Pereda, J. M., García de Lacoba, M., Peyrot, V., Briand, C., Towns Andrews, E., & Bordas, J. (1994) *J. Biol. Chem. 269*, 31785−31792.

Arévalo, M. A., Nieto, J. M., Andreu, D., & Andreu, J. M. (1990) *J. Mol. Biol. 214*, 105−120.

Beese, L., Stubbs, G., & Cohen, C. (1987) *J. Mol. Biol. 194*, 257−264.

Best, D., Warr, P. J., & Gull, K. (1981) *Anal. Biochem. 114*, 281−284.

Bond, J. S. (1989) in *Proteolytic enzymes* (Beynon, R. J., & Bond, J. S., Eds.) pp 233−240, IRL Press, Oxford, U.K.

Breitling, F., & Little, M. (1986) *J. Mol. Biol. 189*, 367−370.

Brown, H. R., & Erickson, H. P. (1983) *Arch. Biochem. Biophys. 220*, 46−51.

de la Viña, S., Andreu, D., Medrano, F. J., Nieto, J. M., & Andreu, J. M. (1988) *Biochemistry 27*, 5352−5365.

de Pereda, J. M., Leynadier, D., Evangelio, J. A., Chacón, P., & Andreu, J. M. (1996) *Biochemistry 35*, 14203−14215.

Díaz, J. F., & Andreu, J. M. (1993) *Biochemistry 32*, 2747−2755.

Díaz, J. F., Menéndez, M., & Andreu, J. M. (1993) *Biochemistry 32*, 10067−10077.

Díaz, J. F., Pantos, E., Bordas, J., & Andreu, J. M. (1994) *J. Mol. Biol. 238*, 214−225.

Díaz, J. F., Andreu, J. M., Diakun, G., Towns-Andrews, E., & Bordas, J. (1996) *Biophys. J. 70*, 2408−2420.

Ebeling, W., Hennrich, N., Klockow, M., Metz, H., Orth, H. D., & Lang, H. (1974) *Eur. J. Biochem. 47*, 91−97.

Fievez, S., & Carlier, M. F. (1993) *FEBS Lett. 316*, 186−190.

Fontana, A., Fassina, G., Vita, C., Dalzoppo, D., Zamai, M., & Zambonin, M. (1986) *Biochemistry 25*, 1847−1851.

Frigon, R. P., & Timasheff, S. N. (1975) *Biochemistry 14*, 4559−4566.

Gundersen, G. G., Kalnoski, M. H., & Bulinski, J. C. (1984) *Cell 36*, 779−789.

Hubbard, S. J., Campbell, S. F., & Thornton, J. M. (1991) *J. Mol. Biol. 220*, 507−530.

Hyman, A. A., Chretien, D., Arnal, I., & Wade, R. H. (1995) *J. Cell Biol. 128*, 117−125.

Kabsch, W., Mannherz, H. G., Suck, D., Pai, E. F., & Holmes, K. C. (1990) *Nature 347*, 37−44.

Kikkawa, M., Ishikawa, T., Wakabayashi, T., & Hirokawa, N. (1995) *Nature 376*, 274−277.

Kirchner, K., & Mandelkow, E. M. (1985) *EMBO J. 4*, 2397−2402.

Krauhs, E., Little, M., Kempf, T., Hofer-Warbinek, R., Ade, W., & Ponstingl, H. (1981) *Proc. Natl. Acad. Sci. U.S.A. 78*, 4156−4160.

Kreis, T. E. (1987) *EMBO J. 6*, 2597−2602.

Kruft, V., & Wittmann-Liebold, B. (1991) *Biochemistry 30*, 11781−11787.

Kull, J. F., Sablin, E. P., Lau, R., Fletterick, R. J., & Vale, R. D. (1996) *Nature 380*, 550−555.

Kumar, N., & Flavin, M. (1981) *J. Biol. Chem. 256*, 7678−7686.

Laemmli, U. K. (1970) *Nature 225*, 680−685.

Laue, T. M., Shah, D. B., Ridgeway, T. M., & Pelletier, S. L. (1993) in *Analytical Ultracentrifugation in Biochemistry and Polymer Science* (Harding, S. E., & Rowe, A. J., Eds.) pp 90−125, Royal Society of Chemistry, U.K.

LeDizet, M., & Piperno, G. (1987) *Proc. Natl. Acad. Sci. U.S.A. 84*, 5720−5724.

Lee, J. C., Frigon, R. P., & Timasheff, S. N. (1973) *J. Biol. Chem. 248*, 7253−7262.

Little, M., & Ludueña, R. F. (1985) *EMBO J. 4*, 51−56.

Lobert, S., & Correia, J. J. (1992) *Arch. Biochem. Biophys. 296*, 152−160.

Lobert, S., Hennington, B. S., & Correia, J. J. (1993) *Cell Motil. Cytoskeleton 25*, 282−297.
Lorenz, M., Popp, D., & Holmes, K. (1993) *J. Mol. Biol. 234*, 826−836.
Ludueña, R. F., Banerjee, A., & Khan, I. A. (1993) *Curr. Opin. Cell Biol. 4*, 53−57.
Mandelkow, E., & Mandelkow, E. M. (1995) *Curr. Opin. Cell Biol. 7*, 72−81.
Mandelkow, E., Thomas, J., & Cohen, C. (1977) *Proc. Natl. Acad. Sci. U.S.A. 74*, 3370−3374.
Mandelkow, E., Mandelkow, E. M., & Bordas, J. (1983) *J. Mol. Biol. 167*, 179−186.
Mandelkow, E. M., Herrmann, M., & Rühl, U. (1985) *J. Mol. Biol. 185*, 311−327.
Matsudaira, P. (1987) *J. Biol. Chem. 262*, 10035−10038.
Monasterio, O., Andreu, J. M., & Lagos, R. (1995) *Comments Mol. Cell. Biophys. 8*, 273−306.
Nogales, E., Wolf, S. G., Khan, I. A., Ludueña, R. F., & Downing, K. H. (1995) *Nature 375*, 424−427.
Paschal, B. M., Obar, R. A., & Vallee, R. B. (1989) *Nature 342*, 569−572.
Peyrot, V., Briand, C., & Andreu, J. M. (1990) *Arch. Biochem. Biophys. 279*, 328−337.
Piperno, G., LeDizet, M., & Chang, X. J. (1987) *J. Cell Biol. 104*, 289−302.
Plyte, S. E., & Kneale, G. G. (1994) *Methods Mol. Biol. 30*, 161−168.
Ponstingl, H., Krauhs, E., Little, M., & Kempf, T. (1981) *Proc. Natl. Acad. Sci. U.S.A. 78*, 2757−2761.
Price, N. C., & Johnson, C. M. (1989) in *Proteolytic enzymes* (Beynon, R. J., & Bond, J. S., Eds.) pp 233−240, IRL Press, Oxford, U.K.
Redecker, V., Melki, R., Promé, D., Le Caer, J. P., & Rossier, J. (1992) *FEBS Lett. 313*, 185−192.
Redecker, V., Levilliers, N., Schmitter, J. M., Le Caer, J. P., Rossier, J., Adoutte, A., & Bré, M. H. (1994) *Science 266*, 1688−1691.
Rüdiger, A., Rüdiger, M., Weber, K., & Schomburg, D. (1995) *Anal. Biochem. 224*, 532−537.
Sablin, E. P., Kull, J. F., Cooke, R., Vale, R. D., & Fletterick, R. J. (1996) *Nature 380*, 555−559.
Sackett, D. L., & Wolff, J. (1986) *J. Biol. Chem. 261*, 9070−9076.
Sackett, D. L., Bhattacharyya, B., & Wolff, J. (1985) *J. Biol. Chem. 260*, 43−45.
Sackett, D. L., Zimmerman, D. A., & Wolff, J. (1989) *Biochemistry 28*, 2662−2666.
Serrano, L., de la Torre, J., Maccioni, R. B., & Avila, J. (1984) *Biochemistry 23*, 4675−4681.
Serrano, L., de la Torre, J., Ludueña, R. F., & Avila, J. (1986) *Arch. Biochem. Biophys. 249*, 611−615.
Sheterline, P., & Sparrow, J. C. (1994) *Protein Profile 1*, 1−121.
Song, Y. H., & Mandelkow, E. (1995) *J. Cell. Biol. 128*, 81−94.
Thompson, W. C. (1982) *Methods Cell Biol. 24*, 235−255.
Vale, R. D., Coppin, C. M., Malik, F., Kull, F. J., & Milligan, R. A. (1994) *J. Biol. Chem. 269*, 23769−23775.
Ward, L. D., Seckler, R., & Timasheff, S. N. (1994) *Biochemistry 33*, 11900−11908.
Weisenberg, R. C., Borisy, G. G., & Taylor, E. (1968) *Biochemistry 7*, 4466−4479.
Wheland, J., & Weber, K. (1987) *J. Cell Sci. 88*, 185−203.
Wheland, J., Willingham, M. K., & Sandoval, I. V. (1983) *J. Cell Biol. 97*, 1467−1475.
White, E. A., Burton, P. R., & Himes, R. H. (1987) *Cell Motil. Cytoskeleton 7*, 39−45.
Wilson, J. E. (1991) *Methods Biochem. Anal. 35*, 207−250.

BI961356J